 CMES, vol.56, no.3, pp.249-301, 2010

Coupled Thermo-Mechanical Analysis of One-Layered and Multilayered Isotropic and Composite Shells

S. Brischetto[1] **and E. Carrera**[2]

Abstract: This work considers the fully coupled thermo-mechanical analysis of one-layered and multilayered isotropic and composite shells. The temperature is assumed a primary variable as the displacement; it is therefore directly obtained from the model and this feature permits the temperature field to be evaluated through the thickness direction. Three problems are analyzed: - static analysis of shells with imposed temperature on the external surfaces; - static analysis of shells subjected to a mechanical load, with the possibility of considering the temperature field effects; - a free vibration problem, with the evaluation of the temperature field effects. In the first problem, imposing a temperature at the top and bottom of the shells, the static response is given in terms of displacements, stresses and temperature field; the proposed method is very promising if compared to a partially coupled thermo-mechanical analysis, where the temperature is only considered as an external load, and the temperature profile must be a priori defined (considering it linear through the thickness direction or calculating it by solving the Fourier heat conduction equation). A mechanical load is applied in the second problem. The fully coupled thermo-mechanical analysis gives smaller displacement values than those obtained with the pure mechanical analysis; the temperature effect is not considered in this latter approach. The third problem is the free vibration analysis of shells. The fully coupled thermo-mechanical models permit the effect of the temperature field to be evaluated: larger frequencies are obtained with respect to the pure mechanical models. Several refined theories with orders of expansion in the thickness direction, for displacements and temperature, from linear to fourth-order are obtained in the framework of Carrera's Unified Formulation. Both equivalent single layer and layer wise approaches are considered for the multilayered shells.

Keywords: one-layered shells; multilayered shells; Carrera's Unified Formula-

[1] Corresponding author: Salvatore Brischetto, Department of Aeronautics and Space Engineering, Politecnico di Torino, Corso Duca degli Abruzzi, 24, 10129 Torino, ITALY. tel: +39.011.564.6869, fax: +39.011.564.6899, e.mail: salvatore.brischetto@polito.it.

[2] Department of Aeronautics and Space Engineering, Politecnico di Torino, Italy

tion; thermo-mechanical coupling; assumed temperature profile; calculated temperature profile; refined two-dimensional theories.

1 Introduction

The effects of heat on the deformation and stresses of solid elastic bodies are considered by the theory of thermoelasticity. Thermoelasticity is a branch of applied mechanics, where the conventional theory of isothermal elasticity is extended to those processes in which deformation and stresses are produced by both mechanical forces and temperature variations. Thermoelastic processes are not totally reversible because the elastic part may be reversed (the deformations caused by heat are theoretically recoverable through cooling), but the thermal part may not be reversed because of the dissipation of energy that takes place during heat transfer. It is well known that a deformation of the body produces changes in its temperature: the effect of the temperature field on the deformation field is not a one-way phenomenon. These features demonstrate that the mechanical and thermal aspects are coupled and inseparable [Nowinski (1978)], and this coupling considerably complicates the computational aspect of solving actual thermoelastic problems. A possible remedy, as suggested in Nowinski's book [Nowinski (1978)], is to discount the coupling and to evaluate the temperature and deformation fields, in this order, separately. The thermoelastic problem, where the temperature and deformation fields are discounted, is here defined as a partially coupled thermo-mechanical problem.

Partially coupled thermo-mechanical models have extensively been employed in the analysis of typical aeronautical structures, which are subject to severe thermal environments, such as high temperatures, high gradients and cyclic changes in temperature. The temperature variations are one of the most important factors for the stress fields that can cause failure of the structures [Librescu and Marzocca (2003a); Librescu and Marzocca (2003b); Noor and Burton (1992)]. Because of these implications, the effects of both high-temperature and mechanical loadings have to be considered in the design process. An accurate description of local stress fields in the layers of multilayered plates and shells becomes mandatory to prevent thermally loaded structure failure mechanisms. Computational models, developed to study the behavior of high-temperature composite plates and shells, make use of the partially coupled thermo-mechanical analysis [Noor and Burton (1992)]. The temperature is only considered as an external load and the temperature profile must be a priori defined: considering it "a priori" through the thickness direction [Wu and Chen (2008); Brischetto and Carrera (2009); Bhaskar et al. (1986); Khare et al. (2003); Khdeir (1996); Birsan (2009); Sladek et al. (2008a); Sladek et al. (2008b)] or calculating it by solving the Fourier heat conduction equation [Carrera (2000); Carrera (2002); Rolfes et al. (1999); Brischetto (2009); Brischetto et al. (2008);

Noorzaei et al. (2009)]. Further works where the temperature profile and/or the heat flux distribution are analytically calculated are Chao et al. (2009), Chen et al. (2008), Feng et al. (2009), Liu et al. (2009), Sladek et al. (2008c), Sladek et al. (2009), Wu et al. (2007) and Zhou et al. (2009). A complete overview, about the assumed temperature profile and the calculated temperature profile in partially coupled thermo-mechanical models has already been given in Brischetto and Carrera (2010).

Brischetto and Carrera (2010) have proposed a fully coupled thermoelastic analysis for plate geometries: both temperature and displacement fields are primary variables in the thermo-mechanical governing equations. The present companion paper extends this fully coupled thermoelastic analysis to shell geometries, in order to investigate the effects of curvature in such problems. This fully coupled analysis permits several problems, which are of particular interest in the aeronautics and space fields to be analyzed, in a very efficient and simple way. Therefore, the case of shells with imposed temperature on the external surfaces is easily solved without the need to a priori define the temperature profile in the thickness direction. The temperature is a primary variable of the problem, and the values of temperature at the top and bottom are directly imposed: the fully coupled thermo-mechanical governing equations directly give the displacements and the temperature through the thickness direction. In order to calculate the displacements, the partially coupled governing equations instead need an a priori temperature profile in the thickness direction to define the thermal load. The other two possible applications of the fully-coupled governing equations are: an external applied mechanical load and the free vibration problem. These two cases are also investigated in this paper, but a relevant simplification is made: the variation in time of the temperature is not considered, and this means that these two problems are investigated at equilibrium conditions. This great simplification will be removed in a future work in order to investigate the evolution in time of temperature, strain and stress in such problems.

In the open literature, a small amount of work has been devoted to the coupled thermo-mechanical analysis of structures (both thermoelastic and thermoplastic analysis), and only few of them give numerical results. Altay and Dökmeci (1996a) have described the physical behaviour of thermoelastic continuum by means of opportune variational principles. The stress equations of motion and the equation of heat conduction have been written as divergence equations. The strain-mechanical displacement relations and Fourier's heat conduction law have been written as gradient equations. The same authors have extended this method to thermopiezoelectric mediums in Altay and Dökmeci (1996b) by simply adding the charge equation of electrostatics in the divergence equations and the electric field-electric potential relations in the gradient equations. Das et al. (1983) have avoided the use of the

thermoelastic potential to solve the general problem of one-dimensional linearized simultaneous equations of thermoelasticity. Displacement and thermal fields have been obtained in the Laplace transformation domain. This method could be very useful in thermoelasticity or other coupled fields.

Some papers about the thermo-mechanical coupling effects in the case of an applied temperature to the structure are Cannarozzi and Ubertini (2001), Cho and Oh (2004), Oh and Cho (2004), Ibrahimbegovic et al. (2005), Lee (2006), Tanaka et al.(1995). Other papers investigate the effects of thermo-mechanical coupling in structures subjected to mechanical loads, see Carrera et al. (2007), Daneshjoo and Ramezani (2002), Daneshjoo and Ramezani (2004), Yang et al. (2006), Adam and Ponthot (2005). Finally, dynamic thermo-mechanical analysis has been considered in the following papers: Altay and Dökmeci (2001), Givoli and Rand (1994), Wilms and Cohen (1985), Wauer (1996), Kosinski and Frischmuth (2001), Trajkovski and Cukic (1999), Yeh (2005). A complete overview about the mentioned papers is given in the companion paper [Brischetto and Carrera (2010)], where they are discussed further.

In the fully coupled thermo-mechanical analysis here extended to one-layered and multilayered shells, displacement and temperature fields are approximated in the thickness direction by several refined two-dimensional theories based on Carrera's Unified Formulation [Carrera (1995); Carrera(2003)]. A preliminary analysis, for only the coupled free vibration problem of layered plates and shells, has already been proposed by the authors in Carrera and Brischetto (2009). In the case of multilayered shells, both equivalent single layer (ESL) and layer wise (LW) approaches have been developed, as secribed in Section 2. The geometrical relations of the shells, in the case of small deformations and constant radii of curvature, are given in Section 3. Constitutive equations, for the coupled thermo-mechanical analysis, have been obtained in Section 4 from thermoelastic enthalpy density, written in a quadratic form for a linear interaction. The principle of virtual displacements (PVD) can be extended to both partially and fully coupled thermo-mechanical analysis, as proposed in Section 5. The multilayered shells are simply supported with applied harmonic loads, therefore closed-form solutions are obtained in Navier form, as discussed in Section 6. The results, concerning the applied temperature case, the imposed mechanical load case and the free vibration problem, are given in Section 7. Section 8 highlights the main conclusions.

2 Carrera's Unified Formulation, CUF

Carrera's Unified Formulation (CUF) [Carrera (1995); Carrera (2003)] permits to obtain, in a unified manner, a large variety of plate/shell theories. According to CUF, the governing equations are written in terms of a few fundamental nuclei

which do not formally depend on the order of expansion N used in the thickness direction and on the description of variables (equivalent single layer (ESL) or layer wise (LW)). The application of a two-dimensional method for shells permits the unknown variables to be expressed as a set of thickness functions that only depend on the thickness coordinate z and the correspondent variable which depends on the in-plane coordinates α and β. The generic variable $\boldsymbol{f}(\alpha,\beta,z)$, for instance a displacement, and its variation $\delta\boldsymbol{f}(\alpha,\beta,z)$ are written therefore according to the following general expansion:

$$\boldsymbol{f}(\alpha,\beta,z) = F_\tau(z)\boldsymbol{f}_\tau(\alpha,\beta)\,, \qquad \delta\boldsymbol{f}(\alpha,\beta,z) = F_s(z)\delta\boldsymbol{f}_s(\alpha,\beta)\,, \qquad (1)$$
$$with \quad \tau,s = 1,\ldots,N\,,$$

where the bold letters denote arrays, (α,β) are the in-plane curvilinear coordinates and z the thickness one. The summing convention, with repeated indexes τ and s, is assumed. The order of expansion N goes from first to fourth-order, and depending on the used thickness functions, a theory can be: ESL, when the variable is assumed for the whole multilayer and a Taylor expansion is employed as the thickness functions $F(z)$; LW, when the variable is considered independent in each layer and a combination of Legendre polynomials are used as the thickness functions $F(z)$. In the thermo-mechanical models, proposed in this work, displacements can be modelled in both ESL or LW form, temperature is always considered in LW form. A two-dimensional thermo-mechanical model is defined therefore as ESL or LW, depending on the choice made for the displacement vector.

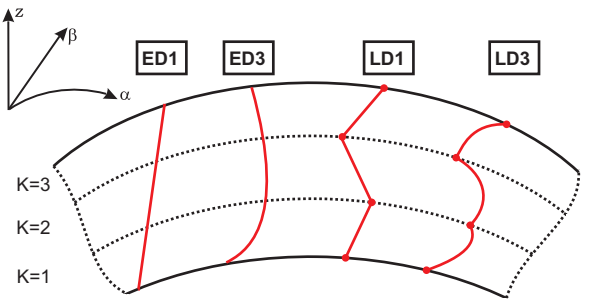

Figure 1: Equivalent Single Layer (ESL) vs. Layer Wise (LW) theories for a multilayered shell.

2.1 Equivalent single layer approach

The displacement $\boldsymbol{u} = (u, v, w)$ is described according to equivalent single layer (ESL) description if the unknowns are the same for the whole multilayered shell [Reddy (2004)] (see Figure 1). The z expansion is obtained via Taylor polynomials, that is:

$$\begin{aligned} u &= F_0\, u_0 + F_1\, u_1 + \ldots + F_N\, u_N = F_\tau\, u_\tau\,, \\ v &= F_0\, v_0 + F_1\, v_1 + \ldots + F_N\, v_N = F_\tau\, v_\tau\,, \\ w &= F_0\, w_0 + F_1\, w_1 + \ldots + F_N\, w_N = F_\tau\, w_\tau\,, \end{aligned} \tag{2}$$

with $\tau = 0, 1, \ldots, N$; N is the order of expansion that ranges from 1 (linear) to 4:

$$F_0 = z^0 = 1,\ F_1 = z^1 = z,\ \ldots,\ F_N = z^N\,. \tag{3}$$

Eq.(2) can be written in a vectorial form:

$$\boldsymbol{u}(\alpha,\beta,z) = F_\tau(z)\boldsymbol{u}_\tau(\alpha,\beta)\,, \qquad \delta\boldsymbol{u}(\alpha,\beta,z) = F_s(z)\delta\boldsymbol{u}_s(\alpha,\beta)\,, \tag{4}$$

$$with \quad \tau, s = 1, \ldots, N\,.$$

Simpler theories, such those which discard the ε_{zz} effect, can be obtained from refined ESL models: it is sufficient to impose that the transverse displacement w is constant in z. First order Shear Deformation Theory (FSDT) [Mindlin (1951)] is obtained from an ESL model with linear expansion in the thickness direction z, by imposing a constant transverse displacement w in z. Classical Lamination Theory (CLT) [Cauchy (1828); Poisson (1829); Kirchhoff (1850)] is obtained from FSDT via an opportune penalty technique which imposes an infinite transverse shear rigidity. All the ESL theories, whit constant or linear transverse displacement w, which means zero or constant transverse normal strain ε_{zz}, show Poisson's locking phenomena: it can be overcame via plane stress conditions in constitutive equations [Carrera and Brischetto (2008a); Carrera and Brischetto (2008b)]

2.2 Layer wise approach

When each layer of a multilayered shell is described as independent shells [Reddy (2004)], a layer wise (LW) approach is accounted for. The displacement $\boldsymbol{u}^k = (u, v, w)^k$ is described for each layer k, in this way the zigzag form of displacement, in multilayered transverse-anisotropy shells, is easily obtained, as indicated in Figure 1. The z expansion for displacement components is made for each layer k:

$$\begin{aligned} u^k &= F_0\, u_0^k + F_1\, u_1^k + \ldots + F_N\, u_N^k = F_\tau\, u_\tau^k\,, \\ v^k &= F_0\, v_0^k + F_1\, v_1^k + \ldots + F_N\, v_N^k = F_\tau\, v_\tau^k\,, \\ w^k &= F_0\, w_0^k + F_1\, w_1^k + \ldots + F_N\, w_N^k = F_\tau\, w_\tau^k\,, \end{aligned} \tag{5}$$

with $\tau = 0,1,\ldots,N$, N is the order of expansion that ranges from 1 (linear) to 4. $k = 1,\ldots,N_l$, where N_l indicates the number of layers. The Eq.(5), written in a vectorial form, is:

$$\boldsymbol{u}^k(\alpha,\beta,z) = F_\tau(z)\boldsymbol{u}^k_\tau(\alpha,\beta)\,, \qquad \delta\boldsymbol{u}^k(\alpha,\beta,z) = F_s(z)\delta\boldsymbol{u}^k_s(\alpha,\beta)\,, \tag{6}$$
$$with \quad \tau,s = t,b,r \quad and \quad k = 1,\ldots,N_l\,,$$

where t and b indicate the top and bottom of each layer k, respectively; r indicates the higher orders of expansion in the thickness direction: $r = 2,\ldots,N$. The thickness functions $F_\tau(\zeta_k)$ and $F_s(\zeta_k)$ have now been defined at the k-layer level, they are a linear combination of Legendre polynomials $P_j = P_j(\zeta_k)$ of the j^{th}-order defined in ζ_k-domain ($\zeta_k = \frac{2z_k}{h_k}$ with z_k local coordinate and h_k thickness, both referred to k^{th} layer, so $-1 \leq \zeta_k \leq 1$). The first five Legendre polynomials are:

$$P_0 = 1,\ P_1 = \zeta_k,\ P_2 = \frac{(3{\zeta_k}^2 - 1)}{2},\ P_3 = \frac{5{\zeta_k}^3}{2} - \frac{3\zeta_k}{2},\ P_4 = \frac{35{\zeta_k}^4}{8} - \frac{15{\zeta_k}^2}{4} + \frac{3}{8}\,, \tag{7}$$

their combinations for the thickness functions are:

$$F_t = F_0 = \frac{P_0 + P_1}{2},\ F_b = F_1 = \frac{P_0 - P_1}{2},\ F_r = P_r - P_{r-2} \quad with \quad r = 2,\ldots,N\,. \tag{8}$$

The chosen functions have the following interesting properties:

$$\zeta_k = 1 \ : \ F_t = 1;\ F_b = 0;\ F_r = 0 \quad at\ top\,, \tag{9}$$
$$\zeta_k = -1 \ : \ F_t = 0;\ F_b = 1;\ F_r = 0 \quad at\ bottom\,, \tag{10}$$

that is interface values of the variables are considered as variable unknowns, see Figure 1. This feature permits to easily imposing the compatibility conditions for displacements at each layer interface. In LW models, even if a linear expansion in z is considered for the transverse displacement w, Poisson's locking phenomena does not appear: the transverse normal strain ε_{zz} is piece-wise constant in the thickness direction [Carrera and Brischetto (2008a); Carrera and Brischetto (2008b)].

In the case of thermo-mechanical problems, the primary variables are the displacement vector $\boldsymbol{u} = (u,v,w)$ and the scalar sovra-temperature θ (temperature T_1 referred to the reference external room temperature T_0, $\theta = T_1 - T_0$). By considering the higher spatial gradient of the temperature field, the variable θ^k is always modelled as LW [Carrera et al. (2007)]:

$$\theta^k(\alpha,\beta,z) = F_\tau(z)\theta^k_\tau(\alpha,\beta)\,, \qquad \delta\theta^k(\alpha,\beta,z) = F_s(z)\delta\theta^k_s(\alpha,\beta)\,, \tag{11}$$
$$with \quad \tau,s = t,b,r \quad and \quad k = 1,\ldots,N_l\,.$$

The thickness functions are a combination of Legendre polynomials as indicated in Eqs.(7) and (8). The sovra-temperature θ can be considered as an external load [Brischetto and Carrera (2009); Brischetto (2009)] or as a primary variable [Brischetto and Carrera (2010); Carrera et al. (2007)]. A two-dimensional model for thermo-mechanical problems is defined as ESL or LW depending on the choice made for the displacement vector: the temperature is always considered in LW form.

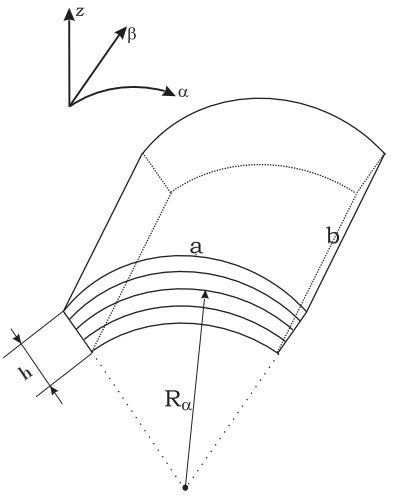

Figure 2: Reference system for a multilayered cylindrical shell.

3 Geometrical relations

We define a thin shell as a three-dimensional body bounded by two closely spaced curved surfaces, the distance between the two surfaces must be small in comparison with the other dimensions. The middle surface of the shell is the locus of points which lie midway between these surfaces. The distance between the surfaces measured along the normal to the middle surface is the *thickness* of the shell at that point [Leissa (1973)]. Geometry and the reference system are indicated in Figure 2. The square of an infinitesimal linear segment in the layer, the associated

infinitesimal area and volume are given by:

$$ds_k^2 = {H_\alpha^k}^2\, d\alpha_k^2 \,+\, {H_\beta^k}^2\, d\beta_k^2 + {H_z^k}^2\, dz_k^2\,, \tag{12}$$

$$d\Omega_k = H_\alpha^k H_\beta^k\, d\alpha_k\, d\beta_k\,, \tag{13}$$

$$dV_k = H_\alpha^k\, H_\beta^k\, H_z^k\, d\alpha_k\, d\beta_k\, dz_k\,, \tag{14}$$

where the metric coefficients are:

$$H_\alpha^k = A^k(1+z_k/R_\alpha^k),\quad H_\beta^k = B^k(1+z_k/R_\beta^k),\quad H_z^k = 1\,. \tag{15}$$

k denotes the k-layer of the multilayered shell; R_α^k and R_β^k are the principal radii of curvature along the coordinates α_k and β_k, respectively. A^k and B^k are the coefficients of the first fundamental form of Ω_k (Γ_k is the Ω_k boundary). In this paper, the attention has been restricted to shells with constant radii of curvature (cylindrical, spherical, toroidal geometries) for which $A^k = B^k = 1$. Details for shells are reported in Leissa (1973). The geometrical relations for shells, in case of thermo-mechanical problems, link the mechanical strains with the displacement vector and the spatial gradient of temperature with the scalar temperature. The relations split in in-plane (p) and out-of-plane (n) components are:

$$\boldsymbol{\varepsilon}_{pG}^k = [\varepsilon_{\alpha\alpha}, \varepsilon_{\beta\beta}, \gamma_{\alpha\beta}]^{kT} = (\boldsymbol{D}_p^k + \boldsymbol{A}_p^k)\, \boldsymbol{u}^k\,, \tag{16}$$

$$\boldsymbol{\varepsilon}_{nG}^k = [\gamma_{\alpha z}, \gamma_{\beta z}, \varepsilon_{zz}]^{kT} = (\boldsymbol{D}_{np}^k + \boldsymbol{D}_{nz}^k - \boldsymbol{A}_n^k)\, \boldsymbol{u}^k\,, \tag{17}$$

$$\boldsymbol{\vartheta}_{pG}^k = [\vartheta_\alpha, \vartheta_\beta]^{kT} = -\boldsymbol{D}_{tp}^k\, \theta^k\,, \tag{18}$$

$$\boldsymbol{\vartheta}_{nG}^k = [\vartheta_z]^k = -\boldsymbol{D}_{tn}^k\, \theta^k\,, \tag{19}$$

$\boldsymbol{\varepsilon}_{pG}^k$ and $\boldsymbol{\varepsilon}_{nG}^k$ are the in-plane and transverse strains, respectively. $\boldsymbol{u}^k = (u,v,w)^k$ is the displacement vector. $\boldsymbol{\vartheta}_{pG}^k$ and $\boldsymbol{\vartheta}_{nG}^k$ are in-plane and transverse spatial gradients of temperature, respectively. θ^k is the scalar temperature referred to the reference external room temperature. T means the transpose of a vector. The explicit form of the introduced arrays follows:

$$\boldsymbol{D}_p^k = \begin{bmatrix} \frac{\partial_{\alpha_k}}{H_\alpha^k} & 0 & 0 \\ 0 & \frac{\partial_{\beta_k}}{H_\beta^k} & 0 \\ \frac{\partial_{\beta_k}}{H_\beta^k} & \frac{\partial_{\alpha_k}}{H_\alpha^k} & 0 \end{bmatrix},\ \boldsymbol{D}_{np}^k = \begin{bmatrix} 0 & 0 & \frac{\partial_{\alpha_k}}{H_\alpha^k} \\ 0 & 0 & \frac{\partial_{\beta_k}}{H_\beta^k} \\ 0 & 0 & 0 \end{bmatrix},\ \boldsymbol{D}_{nz}^k = \begin{bmatrix} \partial_{z_k} & 0 & 0 \\ 0 & \partial_{z_k} & 0 \\ 0 & 0 & \partial_{z_k} \end{bmatrix},$$

$$\boldsymbol{D}_{tp}^k = \begin{bmatrix} \frac{\partial_{\alpha_k}}{H_\alpha^k} \\ \frac{\partial_{\beta_k}}{H_\beta^k} \end{bmatrix},\ \boldsymbol{D}_{tn}^k = \begin{bmatrix} \partial_{z_k} \end{bmatrix}, \tag{20}$$

$$\boldsymbol{A}_p^k = \begin{bmatrix} 0 & 0 & \frac{1}{H_\alpha^k R_\alpha^k} \\ 0 & 0 & \frac{1}{H_\beta^k R_\beta^k} \\ 0 & 0 & 0 \end{bmatrix} , \boldsymbol{A}_n^k = \begin{bmatrix} \frac{1}{H_\alpha^k R_\alpha^k} & 0 & 0 \\ 0 & \frac{1}{H_\beta^k R_\beta^k} & 0 \\ 0 & 0 & 0 \end{bmatrix} . \tag{21}$$

The symbols in differential operators matrices indicate the partial derivatives $\partial_{\alpha_k} = \frac{\partial}{\partial \alpha_k}$, $\partial_{\beta_k} = \frac{\partial}{\partial \beta_k}$ and $\partial_{z_k} = \frac{\partial}{\partial z_k}$. The parameters H_α^k and H_β^k equal 1 in case of plates because the radii of curvature R_α^k and R_β^k are infinite: the pure geometrical contributes $\boldsymbol{A}_p^k$ and $\boldsymbol{A}_n^k$ equal zero in case of plate geometry.

4 Constitutive equations

Constitutive equations, for the thermo-mechanical problem, are obtained in according to that reported in Carrera et al. (2007) and Carrera et al. (2008). The coupling between the mechanical and thermal fields can be determined by using thermodynamical principles and Maxwell's relations [Altay and Dokmeci (1996a); Altay and Dokmeci (1996b); Cannarozzi and Ubertini (2001); Altay and Dokmeci (2001)]. For this aim, it is necessary to define a *Gibbs free-energy function G* and a *thermomechanical enthalpy density H* [Nowinski (1978); Ikeda (1990)]:

$$G(\varepsilon_{ij}, \theta) = \sigma_{ij}\varepsilon_{ij} - \eta\,\theta \,, \tag{22}$$

$$H(\varepsilon_{ij}, \theta, \vartheta_i) = G(\varepsilon_{ij}, \theta) - F(\vartheta_i) \,, \tag{23}$$

where σ_{ij} and ε_{ij} are the stress and strain components. η is the variation of entropy per unit of volume, and θ the sovra-temperature considered with respect to the reference temperature T_0. The function $F(\vartheta_i)$ is the dissipation function, it depends by the spatial temperature gradient ϑ_i:

$$F(\vartheta_i) = \frac{1}{2}\kappa_{ij}\vartheta_i\vartheta_j - \tau_0\dot{h}_i \,, \tag{24}$$

where κ_{ij} is the symmetric, positive semidefinite conductivity tensor. In the second term, τ_0 is a thermal relaxation parameter and $\dot{h}_i$ is the temporal derivative of the heat flux h_i. The thermal relaxation parameter is omitted in the present work. Further details about the dissipation function $F(\vartheta_i)$ can be found in Altay and Dokmeci (1996a), Cannarozzi and Ubertini (2001) and Yang et al. (2006).

The thermomechanical enthalpy density H can be expanded in order to obtain a quadratic form for a linear interaction:

$$H(\varepsilon_{ij}, \theta, \vartheta_i) = \frac{1}{2}Q_{ijkl}\varepsilon_{ij}\varepsilon_{kl} - \lambda_{ij}\varepsilon_{ij}\theta - \frac{1}{2}\chi\theta^2 - \frac{1}{2}\kappa_{ij}\vartheta_i\vartheta_j \,, \tag{25}$$

where Q_{ijkl} is the elastic coefficients tensor considered for an orthotropic material in the problem reference system. λ_{ij} are the thermo-mechanical coupling coefficients, $\chi = \frac{\rho C_v}{T_0}$ where ρ is the material density, C_v is the specific heat per unit mass and T_0 is the reference temperature [Carrera et al. (2007)].

The constitutive equations are obtained by considering the following relations:

$$\sigma_{ij} = \frac{\partial H}{\partial \varepsilon_{ij}} , \quad \eta = -\frac{\partial H}{\partial \theta} , \quad h_i = -\frac{\partial H}{\partial \vartheta_i} . \tag{26}$$

By considering Eqs.(25) and (26), the constitutive equations for the thermo-mechanical problem are obtained:

$$\sigma_{ij} = Q_{ijkl}\varepsilon_{kl} - \lambda_{ij}\theta , \tag{27}$$

$$\eta = \lambda_{ij}\varepsilon_{ij} + \chi\theta , \tag{28}$$

$$h_i = \kappa_{ij}\vartheta_j . \tag{29}$$

Above equations can be written in single-subscript notation by using the indexes $m = q = 1,2,3,4,5,6$ and $i = j = 1,2,3$:

$$\sigma_m = Q_{mq}\varepsilon_q - \lambda_m\theta , \tag{30}$$

$$\eta = \lambda_q\varepsilon_q + \chi\theta , \tag{31}$$

$$h_i = \kappa_{ij}\vartheta_j . \tag{32}$$

From the equations written in single-subscript notations, it is easy to write their matrix form; the matrices and vectors are indicated in bold. Considering a generic multilayered shell, Eqs.(30)-(32) are written for a generic layer k in the problem reference system (α, β, z) as:

$$\boldsymbol{\sigma}^k = \boldsymbol{Q}^k\boldsymbol{\varepsilon}^k - \boldsymbol{\lambda}^k\theta^k , \tag{33}$$

$$\eta^k = \boldsymbol{\lambda}^{kT}\boldsymbol{\varepsilon}^k + \chi^k\theta^k , \tag{34}$$

$$\boldsymbol{h}^k = \boldsymbol{\kappa}^k\boldsymbol{\vartheta}^k , \tag{35}$$

where the sovra-temperature θ^k, the term χ^k and the entropy for unite volume η^k are scalar variables in each layer k. The (6×1) vectors of stress and strain are:

$$\boldsymbol{\sigma}^k = \left\{ \begin{array}{c} \sigma_{\alpha\alpha} \\ \sigma_{\beta\beta} \\ \sigma_{zz} \\ \sigma_{\beta z} \\ \sigma_{\alpha z} \\ \sigma_{\alpha\beta} \end{array} \right\}^k , \quad \boldsymbol{\varepsilon}^k = \left\{ \begin{array}{c} \varepsilon_{\alpha\alpha} \\ \varepsilon_{\beta\beta} \\ \varepsilon_{zz} \\ \gamma_{\beta z} \\ \gamma_{\alpha z} \\ \gamma_{\alpha\beta} \end{array} \right\}^k . \tag{36}$$

The (3×1) vectors of heat flux $\boldsymbol{h}^k$ and spatial gradient of temperature $\boldsymbol{\vartheta}^k$ are:

$$\boldsymbol{h}^k = \left\{ \begin{array}{c} h_\alpha \\ h_\beta \\ h_z \end{array} \right\}^k , \quad \boldsymbol{\vartheta}^k = \left\{ \begin{array}{c} \vartheta_\alpha \\ \vartheta_\beta \\ \vartheta_z \end{array} \right\}^k . \tag{37}$$

The (6×1) array of thermo-mechanical coupling coefficients $\boldsymbol{\lambda}^k$ is:

$$\boldsymbol{\lambda}^k = \boldsymbol{Q}^k \, \boldsymbol{\alpha}^k = \left\{ \begin{array}{c} \lambda_1 \\ \lambda_2 \\ \lambda_3 \\ 0 \\ 0 \\ \lambda_6 \end{array} \right\}^k , \tag{38}$$

where the elastic coefficients matrix $\boldsymbol{Q}^k$ of Hooke law, in problem reference system for an orthotropic material [Reddy (2004)], is:

$$\boldsymbol{Q}^k = \left[\begin{array}{cccccc} Q_{11} & Q_{12} & Q_{13} & 0 & 0 & Q_{16} \\ Q_{12} & Q_{22} & Q_{23} & 0 & 0 & Q_{26} \\ Q_{13} & Q_{23} & Q_{33} & 0 & 0 & Q_{36} \\ 0 & 0 & 0 & Q_{44} & Q_{45} & 0 \\ 0 & 0 & 0 & Q_{45} & Q_{55} & 0 \\ Q_{16} & Q_{26} & Q_{36} & 0 & 0 & Q_{66} \end{array} \right]^k , \tag{39}$$

the vector $\boldsymbol{\alpha}^k$ has dimension (6×1) and it contains the thermal expansion coefficients:

$$\boldsymbol{\alpha}^k = \left\{ \begin{array}{c} \alpha_1 \\ \alpha_2 \\ \alpha_3 \\ 0 \\ 0 \\ 0 \end{array} \right\}^k . \tag{40}$$

The matrix $\boldsymbol{\kappa}^k$ of conductivity coefficients has dimension (3×3):

$$\boldsymbol{\kappa}^k = \left[\begin{array}{ccc} \kappa_{11} & \kappa_{12} & 0 \\ \kappa_{12} & \kappa_{22} & 0 \\ 0 & 0 & \kappa_{33} \end{array} \right]^k . \tag{41}$$

In order to use the relations given in Eqs.(33)-(35) in the proposed variational statements, that will be presented in the next section, it is convenient to split them

in in-plane components (subscript p) and out-of-plane components (subscript n). Other two new subscripts are introduced: the subscript C for those variables, in the variational statements, which need the substitution of constitutive equations; the subscript G for those variables, in constitutive equations, which need the substitution of geometrical relations (see Section 3). The split stress and strain components vectors are:

$$\boldsymbol{\sigma}_{pC}^{k} = \left\{ \begin{array}{c} \sigma_{\alpha\alpha} \\ \sigma_{\beta\beta} \\ \sigma_{\alpha\beta} \end{array} \right\}^{k}, \quad \boldsymbol{\sigma}_{nC}^{k} = \left\{ \begin{array}{c} \sigma_{\alpha z} \\ \sigma_{\beta z} \\ \sigma_{zz} \end{array} \right\}^{k}, \quad \boldsymbol{\varepsilon}_{pG}^{k} = \left\{ \begin{array}{c} \varepsilon_{\alpha\alpha} \\ \varepsilon_{\beta\beta} \\ \gamma_{\alpha\beta} \end{array} \right\}^{k}, \quad \boldsymbol{\varepsilon}_{nG}^{k} = \left\{ \begin{array}{c} \gamma_{\alpha z} \\ \gamma_{\beta z} \\ \varepsilon_{zz} \end{array} \right\}^{k}. \tag{42}$$

The vectors (3×1) of heat flux and spatial gradient of the temperature, split in in-plane and out-of-plane components, are:

$$\boldsymbol{h}_{pC}^{k} = \left\{ \begin{array}{c} h_{\alpha} \\ h_{\beta} \end{array} \right\}^{k}, \quad \boldsymbol{h}_{nC}^{k} = \left\{ \begin{array}{c} h_{z} \end{array} \right\}^{k}, \quad \boldsymbol{\vartheta}_{pG}^{k} = \left\{ \begin{array}{c} \vartheta_{\alpha} \\ \vartheta_{\beta} \end{array} \right\}^{k}, \quad \boldsymbol{\vartheta}_{nG}^{k} = \left\{ \begin{array}{c} \vartheta_{z} \end{array} \right\}^{k}. \tag{43}$$

By considering Eqs.(42) and (43), the split form of Eqs.(33)-(35) is:

$$\boldsymbol{\sigma}_{pC}^{k} = \boldsymbol{Q}_{pp}^{k} \boldsymbol{\varepsilon}_{pG}^{k} + \boldsymbol{Q}_{pn}^{k} \boldsymbol{\varepsilon}_{nG}^{k} - \boldsymbol{\lambda}_{p}^{k} \theta^{k}, \tag{44}$$

$$\boldsymbol{\sigma}_{nC}^{k} = \boldsymbol{Q}_{np}^{k} \boldsymbol{\varepsilon}_{pG}^{k} + \boldsymbol{Q}_{nn}^{k} \boldsymbol{\varepsilon}_{nG}^{k} - \boldsymbol{\lambda}_{n}^{k} \theta^{k}, \tag{45}$$

$$\eta_{C}^{k} = \boldsymbol{\lambda}_{p}^{kT} \boldsymbol{\varepsilon}_{pG}^{k} + \boldsymbol{\lambda}_{n}^{kT} \boldsymbol{\varepsilon}_{nG}^{k} + \chi^{k} \theta^{k}, \tag{46}$$

$$\boldsymbol{h}_{p}^{k} = \boldsymbol{\kappa}_{pp}^{k} \boldsymbol{\vartheta}_{pG}^{k} + \boldsymbol{\kappa}_{pn}^{k} \boldsymbol{\vartheta}_{nG}^{k}, \tag{47}$$

$$\boldsymbol{h}_{n}^{k} = \boldsymbol{\kappa}_{np}^{k} \boldsymbol{\vartheta}_{pG}^{k} + \boldsymbol{\kappa}_{nn}^{k} \boldsymbol{\vartheta}_{nG}^{k}. \tag{48}$$

The explicit forms of the split matrices in Eqs.(44)-(48) are:

- Stiffness matrices:

$$\boldsymbol{Q}_{pp}^{k} = \left[\begin{array}{ccc} Q_{11} & Q_{12} & Q_{16} \\ Q_{12} & Q_{22} & Q_{26} \\ Q_{16} & Q_{26} & Q_{66} \end{array} \right]^{k}, \quad \boldsymbol{Q}_{pn}^{k} = \left[\begin{array}{ccc} 0 & 0 & Q_{13} \\ 0 & 0 & Q_{23} \\ 0 & 0 & Q_{36} \end{array} \right]^{k}, \tag{49}$$

$$\boldsymbol{Q}_{np}^{k} = \left[\begin{array}{ccc} 0 & 0 & 0 \\ 0 & 0 & 0 \\ Q_{13} & Q_{23} & Q_{36} \end{array} \right]^{k}, \quad \boldsymbol{Q}_{nn}^{k} = \left[\begin{array}{ccc} Q_{55} & Q_{45} & 0 \\ Q_{45} & Q_{44} & 0 \\ 0 & 0 & Q_{33} \end{array} \right]^{k}.$$

- Thermo-mechanical coupling coefficients:

$$\boldsymbol{\lambda}_{p}^{k} = \left[\begin{array}{c} \lambda_{1} \\ \lambda_{2} \\ \lambda_{6} \end{array} \right]^{k}, \quad \boldsymbol{\lambda}_{n}^{k} = \left[\begin{array}{c} 0 \\ 0 \\ \lambda_{3} \end{array} \right]^{k}. \tag{50}$$

- Conductivity coefficients:

$$\boldsymbol{\kappa}_{pp}^{k} = \begin{bmatrix} \kappa_{11} & \kappa_{12} \\ \kappa_{12} & \kappa_{22} \end{bmatrix}^{k}, \quad \boldsymbol{\kappa}_{pn}^{k} = \begin{bmatrix} 0 \\ 0 \end{bmatrix}^{k}, \tag{51}$$

$$\boldsymbol{\kappa}_{np}^{k} = \begin{bmatrix} 0 & 0 \end{bmatrix}^{k}, \quad \boldsymbol{\kappa}_{nn}^{k} = \begin{bmatrix} \kappa_{33} \end{bmatrix}^{k}.$$

5 Considered variational statements

In this section two different extensions of the Principle of Virtual Displacements (PVD) are given: the first is for the partially coupled thermo-mechanical analysis, the second one is for the fully coupled thermo-mechanical problem. In the case of a partially coupled analysis the PVD is the same of the mechanical case, but the stresses are considered as an algebraic addition of the pure mechanical and pure thermal parts [Brischetto and Carrera (2009); Brischetto (2009)]. For the fully coupled analysis, the virtual internal thermal work is added to the virtual internal mechanical one [Carrera et al. (2007); Carrera et al. (2008)].

5.1 PVD for the partially coupled thermo-mechanical case

In the case of the thermal stress analysis of shells, a possible extension of the PVD considers the temperature as an external load without any coupling between the mechanical and thermal fields [Carrera (2002)]. In the variational statement obtained in Eq.(54) the stresses are seen as an algebraic addition of mechanical (d) and thermal (t) contributions:

$$\boldsymbol{\sigma}_{pC}^{k} = \boldsymbol{\sigma}_{pd}^{k} - \boldsymbol{\sigma}_{pt}^{k} = \boldsymbol{Q}_{pp}^{k}\boldsymbol{\varepsilon}_{pG}^{k} + \boldsymbol{Q}_{pn}^{k}\boldsymbol{\varepsilon}_{nG}^{k} - \boldsymbol{\lambda}_{p}^{k}\theta^{k}, \tag{52}$$

$$\boldsymbol{\sigma}_{nC}^{k} = \boldsymbol{\sigma}_{nd}^{k} - \boldsymbol{\sigma}_{nt}^{k} = \boldsymbol{Q}_{np}^{k}\boldsymbol{\varepsilon}_{pG}^{k} + \boldsymbol{Q}_{nn}^{k}\boldsymbol{\varepsilon}_{nG}^{k} - \boldsymbol{\lambda}_{n}^{k}\theta^{k}, \tag{53}$$

where the arrays $\boldsymbol{\lambda}_p$ and $\boldsymbol{\lambda}_n$ permit the partial coupling between the mechanical field and the temperature.

By considering a laminate of N_l layers, and the integral on the volume V_k of each layer k as an integral on the in plane domain Ω_k plus the integral in the thickness-direction domain A_k, it is possible to write:

$$\sum_{k=1}^{N_l} \int_{\Omega_k} \int_{A_k} \left\{ \delta\boldsymbol{\varepsilon}_{pG}^{k\,T}(\boldsymbol{\sigma}_{pd}^{k} - \boldsymbol{\sigma}_{pt}^{k}) + \delta\boldsymbol{\varepsilon}_{nG}^{k\,T}(\boldsymbol{\sigma}_{nd}^{k} - \boldsymbol{\sigma}_{nt}^{k}) \right\} d\Omega_k dz = \sum_{k=1}^{N_l} \delta L_e^k - \sum_{k=1}^{N_l} \delta L_{in}^k, \tag{54}$$

where δL_e^k and δL_{in}^k are the external and inertial virtual works at the k-layer level, respectively. By substituting the Eqs.(52) and (53) in the variational statement of

Eq.(54), and considering the geometrical relations for shells of Section 3, and the CUF of Section 2, for a generic layer k it is possible to write:

$$\int_{\Omega_k}\int_{A_k}\Big[\Big((\boldsymbol{D}_p^k+\boldsymbol{A}_p^k)\,F_s\delta\boldsymbol{u}_s^k\Big)^T\Big(\boldsymbol{Q}_{pp}^k(\boldsymbol{D}_p^k+\boldsymbol{A}_p^k)\,F_\tau\boldsymbol{u}_\tau^k+\boldsymbol{Q}_{pn}^k(\boldsymbol{D}_{np}^k+\boldsymbol{D}_{nz}^k-\boldsymbol{A}_n^k)F_\tau\boldsymbol{u}_\tau^k-\boldsymbol{\lambda}_p^kF_\tau\theta_\tau^k\Big)+$$
$$\Big((\boldsymbol{D}_{np}^k+\boldsymbol{D}_{nz}^k-\boldsymbol{A}_n^k)F_s\delta\boldsymbol{u}_s^k\Big)^T\Big(\boldsymbol{Q}_{np}^k(\boldsymbol{D}_p^k+\boldsymbol{A}_p^k)\,F_\tau\boldsymbol{u}_\tau^k+\boldsymbol{Q}_{nn}^k(\boldsymbol{D}_{np}^k+\boldsymbol{D}_{nz}^k-\boldsymbol{A}_n^k)F_\tau\boldsymbol{u}_\tau^k \tag{55}$$
$$-\boldsymbol{\lambda}_n^kF_\tau\theta_\tau^k\Big)\Big]d\Omega_kdz=\delta L_e^k-\delta L_{in}^k\,.$$

By using the integration by parts, as given in Brischetto (2009), the governing equations are written in the following compact form:

$$\delta\boldsymbol{u}_s^k:\qquad\boldsymbol{K}_{uu}^{k\tau s}\,\boldsymbol{u}_\tau^k=-\boldsymbol{M}_{uu}^{k\tau s}\,\ddot{\boldsymbol{u}}_\tau^k-\boldsymbol{K}_{u\theta}^{k\tau s}\,\theta_\tau^k+\boldsymbol{p}_{us}^k\,, \tag{56}$$

with related boundary conditions on the layer edge Γ_k:

$$\boldsymbol{\Pi}_{uu}^{k\tau s}\,\boldsymbol{u}_\tau^k-\boldsymbol{\Pi}_{u\theta}^{k\tau s}\,\theta_\tau^k=\boldsymbol{\Pi}_{uu}^{k\tau s}\,\bar{\boldsymbol{u}}_\tau^k-\boldsymbol{\Pi}_{u\theta}^{k\tau s}\,\bar{\theta}_\tau^k\,, \tag{57}$$

where ($-\boldsymbol{K}_{u\theta}^{k\tau s}\theta_\tau^k$) is the thermal load $\boldsymbol{p}_{\theta s}^k$, ($-\boldsymbol{M}_{uu}^{k\tau s}\ddot{\boldsymbol{u}}_\tau^k$) is the inertial load and $\boldsymbol{p}_{us}^k$ is the external mechanical one. From Eqs.(56) and (57), simply discarding the thermal contribution, it is possible to obtain the governing equations and the boundary conditions for the pure mechanical case: the variational statement for this case is obtained from Eq.(54) simply discarding the thermal contribution for the stresses. $\boldsymbol{M}_{uu}^{k\tau s}$ is the inertial contribution in term of fundamental nucleus, $\boldsymbol{u}_\tau^k$ is the vector of the degrees of freedom for the displacements, θ_τ^k is the vector of the degrees of freedom for the sovra-temperature, $\ddot{\boldsymbol{u}}_\tau^k$ is the second temporal derivative of $\boldsymbol{u}_\tau^k$, $\boldsymbol{K}_{uu}^{k\tau s}$ is the fundamental nucleus for the stiffness matrix, $\boldsymbol{K}_{u\theta}^{k\tau s}$ is the fundamental nucleus for the thermal load. $\boldsymbol{\Pi}_{uu}^{k\tau s}$ and $\boldsymbol{\Pi}_{u\theta}^{k\tau s}$ are the fundamental nuclei for the boundary

conditions. These assume the following form:

$$\boldsymbol{K}_{uu}^{k\tau s} = \int_{A_k} \Big[\Big(-\boldsymbol{D}_p^k + \boldsymbol{A}_p^k \Big)^T \Big(\boldsymbol{Q}_{pp}^k (\boldsymbol{D}_p^k + \boldsymbol{A}_p^k) + \boldsymbol{Q}_{pn}^k (\boldsymbol{D}_{np}^k + \boldsymbol{D}_{nz}^k - \boldsymbol{A}_n^k) \Big) + \tag{58}$$

$$\Big(-\boldsymbol{D}_{np}^k + \boldsymbol{D}_{nz}^k - \boldsymbol{A}_n^k \Big)^T \Big(\boldsymbol{Q}_{np}^k (\boldsymbol{D}_p^k + \boldsymbol{A}_p^k) + \boldsymbol{Q}_{nn}^k (\boldsymbol{D}_{np}^k + \boldsymbol{D}_{nz}^k - \boldsymbol{A}_n^k) \Big) \Big] F_s F_\tau H_\alpha^k H_\beta^k dz \,,$$

$$\boldsymbol{K}_{u\theta}^{k\tau s} = \int_{A_k} \Big[\Big(-\boldsymbol{D}_p^k + \boldsymbol{A}_p^k \Big)^T \Big(-\boldsymbol{\lambda}_p^k \Big) + \Big(-\boldsymbol{D}_{np}^k + \boldsymbol{D}_{nz}^k - \boldsymbol{A}_n^k \Big)^T \Big(-\boldsymbol{\lambda}_n^k \Big) \Big] F_s F_\tau H_\alpha^k H_\beta^k dz \,, \tag{59}$$

$$\boldsymbol{M}_{uu}^{k\tau s} = \int_{A_k} (\rho^k \boldsymbol{I}) F_s F_\tau H_\alpha^k H_\beta^k dz \,, \tag{60}$$

$$\boldsymbol{\Pi}_{uu}^{k\tau s} = \int_{A_k} \Big[\boldsymbol{I}_p^{kT} \Big(\boldsymbol{Q}_{pp}^k (\boldsymbol{D}_p^k + \boldsymbol{A}_p^k) + \boldsymbol{Q}_{pn}^k (\boldsymbol{D}_{np}^k + \boldsymbol{D}_{nz}^k - \boldsymbol{A}_n^k) \Big) + \boldsymbol{I}_{np}^{kT} \Big(\boldsymbol{Q}_{np}^k (\boldsymbol{D}_p^k + \boldsymbol{A}_p^k) + \tag{61}$$

$$\boldsymbol{Q}_{nn}^k (\boldsymbol{D}_{np}^k + \boldsymbol{D}_{nz}^k - \boldsymbol{A}_n^k) \Big) \Big] F_s F_\tau H_\alpha^k H_\beta^k dz \,,$$

$$\boldsymbol{\Pi}_{u\theta}^{k\tau s} = \int_{A_k} \Big[\boldsymbol{I}_p^{kT} \Big(-\boldsymbol{\lambda}_p^k \Big) + \boldsymbol{I}_{np}^{kT} \Big(-\boldsymbol{\lambda}_n^k \Big) \Big] F_s F_\tau H_\alpha^k H_\beta^k dz \,. \tag{62}$$

ρ^k is the mass density of the k^{th} layer and $\boldsymbol{I}$ is the (3×3) identity matrix. $\boldsymbol{I}_p^k$ and $\boldsymbol{I}_{np}^k$ are (3×3) matrices, to perform the integration by parts, obtained from matrices $\boldsymbol{D}_p^k$ and $\boldsymbol{D}_{np}^k$ simply replacing the differential operators with 1.

In order to define the thermal load, the temperature profile must be a priori given: by linearly assuming it in the thickness direction (θ_a) or by calculating it with solving the Fourier heat conduction equation (θ_c).

5.1.1 Assumed temperature profile, θ_a

If the values of the temperature are known at the top and bottom surfaces of the shell, an assumed profile $\theta(z)$, which varies linearly from the top to the bottom, is given. The temperature is assumed bi-sinusoidal in the plane (α, β) at the top and bottom shell surfaces:

$$\theta(\alpha, \beta, z) = \hat{\theta}(z) \sin(\frac{m\pi}{a}\alpha) \sin(\frac{n\pi}{b}\beta) \,, \tag{63}$$

with values $\hat{\theta}(+h/2) = \theta_t$ and $\hat{\theta}(-h/2) = \theta_b$. a and b are the shell dimensions. m and n are the waves number. In the case of assumed temperature profile (θ_a) a linear through the thickness distribution is considered from θ_t to θ_b. Independently by

the number of considered layers, the linear profile is always the same as indicated in Figure 3: here examples of one-layered, two-layered and three-layered shells are given for a temperature profile which goes from $+1.0$ at the top to 0.0 at the bottom. The temperature profile is approximated as displacements in case of the LW approach:

$$\theta^k(z) = F_\tau \, \theta^k_\tau \qquad \text{with} \quad \tau = t, b, r \quad \text{and} \quad r = 2, \ldots, 4 \,, \tag{64}$$

t and b indicate the top and bottom of the considered k^{th} layer. The thickness functions F_τ are a combination of Legendre polynomials (see Section 2.2).

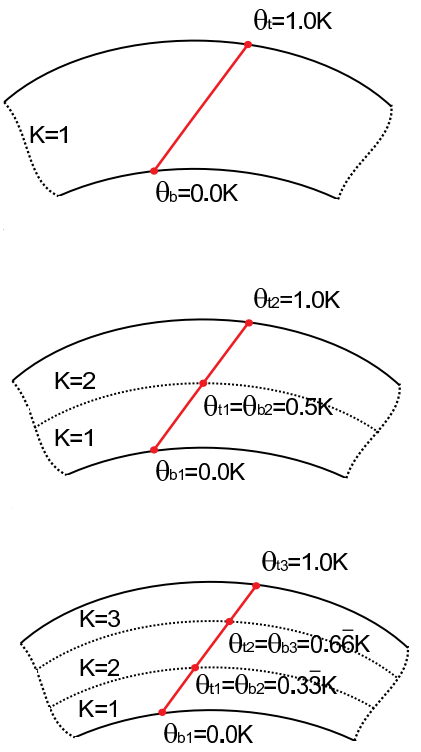

Figure 3: Assumed linear sovra-temperature profile (θ_a) through the thickness direction of the one-layered, two-layered and three-layered shell, respectively.

If the temperature is assumed linear through the thickness, the values at the top and bottom surfaces, and therefore F_t and F_b, would be sufficient to describe the assumed profile via CUF (see Figure 3) [Brischetto and Carrera (2009)].

5.1.2 Calculated temperature profile, θ_c

The calculation procedure for the actual temperature profile in case of one or more layers is given in Carrera (2002), Brischetto (2009) and Brischetto et al. (2008), in order to obtain the values of θ_τ^k for the Eq.(64). The Fourier heat conduction equation in curvilinear coordinates is:

$$(\frac{\kappa_{11}^k}{{H_\alpha^k}^2})\,\frac{\partial^2\theta}{\partial\alpha^2}+(\frac{\kappa_{22}^k}{{H_\beta^k}^2})\,\frac{\partial^2\theta}{\partial\beta^2}+\kappa_{33}^k\,\frac{\partial^2\theta}{\partial z^2}=0\,, \tag{65}$$

κ_{11}^k, κ_{22}^k and κ_{33}^k are the thermal conductivities along the three shell directions α, β and z. $H_\alpha^k=(1+z^k/R_\alpha^k)$ and $H_\beta^k=(1+z^k/R_\beta^k)$ are the metric coefficients. In the case of plates the Eq.(65) has $H_\alpha^k=H_\beta^k=1$ and the coefficients κ_{11}^k, κ_{22}^k and κ_{33}^k are constant. In the case of shells, we can define three new coefficients $\kappa_{11}^{*k}=\frac{\kappa_{11}^k}{{H_\alpha^k}^2}$, $\kappa_{22}^{*k}=\frac{\kappa_{22}^k}{{H_\beta^k}^2}$ and $\kappa_{33}^{*k}=\kappa_{33}^k$, that in a generic layer k depend on the thickness coordinate of the shell:

$$\kappa_{11}^{*k}\,\frac{\partial^2\theta}{\partial\alpha^2}+\kappa_{22}^{*k}\,\frac{\partial^2\theta}{\partial\beta^2}+\kappa_{33}^{*k}\,\frac{\partial^2\theta}{\partial z^2}=0\,. \tag{66}$$

The Eq.(66) has not constant coefficients in the layer k because of curvatures. It can be solved by introducing, for each layer k, a given number of mathematical layers (N_{ml}). It is solved in the case of shell subjected to a bi-sinusoidal temperature at the top and at the bottom. The thermal boundary conditions are:

$$\begin{aligned}
&\theta=0 \qquad \text{at} \quad \alpha=0,a \quad \text{and} \quad \beta=0,b\,,\\
&\theta=\theta_b\,\sin\left(\frac{m\pi\alpha}{a}\right)\,\sin\left(\frac{n\pi\beta}{b}\right) \qquad \text{at} \quad z=-\frac{h}{2} \quad \text{with} \quad b:\ \text{bottom}\,,\\
&\theta=\theta_t\,\sin\left(\frac{m\pi\alpha}{a}\right)\,\sin\left(\frac{n\pi\beta}{b}\right) \qquad \text{at} \quad z=+\frac{h}{2} \quad \text{with} \quad t:\ \text{top}\,,
\end{aligned} \tag{67}$$

where m and n are the waves number along the two in-plane shell directions (α,β). a and b are the shell dimensions, h is the shell thickness, and θ_b and θ_t are the amplitudes of the temperature at the bottom and top of each layer, respectively.

We compute the temperature θ_c at different values z_N in the thickness of the multilayered shell by solving the Eq.(66) with the boundary conditions in Eq.(67). By

solving the system in Eq.(68), we obtain the N values of θ_τ^k for the CUF:

$$\begin{bmatrix} \theta_c(z_1) \\ \theta_c(z_2) \\ \vdots \\ \theta_c(z_N) \end{bmatrix} = \begin{bmatrix} F_0(z_1) & F_1(z_1) & \cdots & F_N(z_1) \\ F_0(z_2) & F_1(z_2) & \cdots & F_N(z_2) \\ \vdots & \vdots & \vdots & \vdots \\ F_0(z_N) & F_1(z_N) & \cdots & F_N(z_N) \end{bmatrix} \begin{bmatrix} \theta_0^k \\ \theta_1^k \\ \vdots \\ \theta_N^k \end{bmatrix} . \tag{68}$$

Therefore, if we consider a generic multilayered shell, the temperature profile is approximated by Eq.(64) and the N values of θ_τ^k are given by Eq.(68). The details, here omitted for sake of brevity, can be found in Carrera (2002), Brischetto (2009) and Brischetto et al. (2008).

5.2 PVD for the fully coupled thermo-mechanical case

In case of fully coupling between the thermal and mechanical fields, the variational statement is the PVD with the introduction of the virtual internal thermal work. This variational statement is:

$$\int_V \left(\delta \boldsymbol{\varepsilon}_{pG}^T \boldsymbol{\sigma}_{pC} + \delta \boldsymbol{\varepsilon}_{nG}^T \boldsymbol{\sigma}_{nC} - \delta\theta\, \eta_C - \delta \boldsymbol{\vartheta}_{pG}^T \boldsymbol{h}_{pC} - \delta \boldsymbol{\vartheta}_{nG}^T \boldsymbol{h}_{nC} \right) dV = \delta L_e - \delta L_{in} \, . \tag{69}$$

By considering a laminate of N_l layers and the volume V_k for each layer k as an integral on the in-plane surface Ω_k and an integral in the thickness direction domain A_k, the Eq.(69) can be rewritten as:

$$\sum_{k=1}^{N_l} \int_{\Omega_k} \int_{A_k} \left\{ \delta \boldsymbol{\varepsilon}_{pG}^k{}^T \boldsymbol{\sigma}_{pC}^k + \delta \boldsymbol{\varepsilon}_{nG}^k{}^T \boldsymbol{\sigma}_{nC}^k - \delta\theta^k \eta_C^k - \delta \boldsymbol{\vartheta}_{pG}^k{}^T \boldsymbol{h}_{pC}^k - \delta \boldsymbol{\vartheta}_{nG}^k{}^T \boldsymbol{h}_{nC}^k \right\} d\Omega_k dz$$
$$= \sum_{k=1}^{N_l} \delta L_e^k - \sum_{k=1}^{N_l} \delta L_{in}^k \, , \tag{70}$$

where δL_e^k and δL_{in}^k are the external and inertial virtual work at the k-layer level, respectively.

The governing equations have the following form:

$$\begin{aligned} \delta \boldsymbol{u}_s^k : \quad & \boldsymbol{K}_{uu}^{k\tau s}\, \boldsymbol{u}_\tau^k + \boldsymbol{K}_{u\theta}^{k\tau s}\, \theta_\tau^k = \boldsymbol{p}_{us}^k - \boldsymbol{M}_{uu}^{k\tau s}\, \ddot{\boldsymbol{u}}_\tau^k \\ \delta \theta_s^k : \quad & \boldsymbol{K}_{\theta u}^{k\tau s}\, \boldsymbol{u}_\tau^k + \boldsymbol{K}_{\theta\theta}^{k\tau s}\, \theta_\tau^k = \boldsymbol{p}_{\theta s}^k \, . \end{aligned} \tag{71}$$

The arrays $\boldsymbol{p}_{us}^k$ and $\boldsymbol{p}_{\theta s}^k$ indicate the variationally consistent mechanical and thermal loadings, respectively. Along with these governing equations the following

boundary conditions on the edge Γ_k of the in-plane integration domain Ω_k hold:

$$\begin{aligned}
&\mathbf{\Pi}^{k\tau s}_{uu}\ \boldsymbol{u}^k_\tau + \mathbf{\Pi}^{k\tau s}_{u\theta}\ \theta^k_\tau = \ \mathbf{\Pi}^{k\tau s}_{uu}\ \bar{\boldsymbol{u}}^k_\tau + \mathbf{\Pi}^{k\tau s}_{u\theta}\ \bar{\theta}^k_\tau \\
&\mathbf{\Pi}^{k\tau s}_{\theta u}\ \boldsymbol{u}^k_\tau + \mathbf{\Pi}^{k\tau s}_{\theta\theta}\ \theta^k_\tau = \mathbf{\Pi}^{k\tau s}_{\theta u}\ \bar{\boldsymbol{u}}^k_\tau + \mathbf{\Pi}^{k\tau s}_{\theta\theta}\ \bar{\theta}^k_\tau \ .
\end{aligned} \tag{72}$$

As indicated in Carrera et al. (2007), the sovra-temperature θ^k is a variable of the problem. The displacements $\boldsymbol{u}^k$ can be seen in ESL or LW form. Independently by the choice made for the displacements, the sovra-temperature is always seen in LW form.

As discussed in Altay and Dokmeci (1996b) and Cannarozzi and Ubertini (2001), the variational statement includes only the internal thermal work made by the gradient of temperature in the case of applied temperature at the top and bottom of the structure; it includes only the internal thermal work made by the temperature in the case of applied mechanical load on the structure or free vibration problem.

5.2.1 Imposed temperature on the top/bottom shell surfaces

In the case of temperature imposed at the top and bottom of the structure, in the Eq.(70) the term $\delta\theta^k\eta^k_C$ is not considered because it does not exist a virtual variation of temperature. Therefore, the variational statement is:

$$\sum_{k=1}^{N_l} \int_{\Omega_k}\int_{A_k} \left\{ \delta\boldsymbol{\varepsilon}^k_{pG}{}^T \boldsymbol{\sigma}^k_{pC} + \delta\boldsymbol{\varepsilon}^k_{nG}{}^T \boldsymbol{\sigma}^k_{nC} - \delta\boldsymbol{\vartheta}^k_{pG}{}^T \boldsymbol{h}^k_{pC} - \delta\boldsymbol{\vartheta}^k_{nG}{}^T \boldsymbol{h}^k_{nC} \right\} d\Omega_k dz = \sum_{k=1}^{N_l} \delta L^k_e \ . \tag{73}$$

From the constitutive equations, as obtained in Eqs.(44)-(48), simply discarding the entropy η^k_c:

$$\boldsymbol{\sigma}^k_{pC} = \boldsymbol{Q}^k_{pp}\boldsymbol{\varepsilon}^k_{pG} + \boldsymbol{Q}^k_{pn}\boldsymbol{\varepsilon}^k_{nG} - \boldsymbol{\lambda}^k_p\theta^k \ , \tag{74}$$

$$\boldsymbol{\sigma}^k_{nC} = \boldsymbol{Q}^k_{np}\boldsymbol{\varepsilon}^k_{pG} + \boldsymbol{Q}^k_{nn}\boldsymbol{\varepsilon}^k_{nG} - \boldsymbol{\lambda}^k_n\theta^k \ , \tag{75}$$

$$\boldsymbol{h}^k_{pC} = \boldsymbol{\kappa}^k_{pp}\boldsymbol{\vartheta}^k_{pG} + \boldsymbol{\kappa}^k_{pn}\boldsymbol{\vartheta}^k_{nG} \ , \tag{76}$$

$$\boldsymbol{h}^k_{nC} = \boldsymbol{\kappa}^k_{np}\boldsymbol{\vartheta}^k_{pG} + \boldsymbol{\kappa}^k_{nn}\boldsymbol{\vartheta}^k_{nG} \ . \tag{77}$$

The geometrical relations for shells have been obtained in Section 3, and Carrera's Unified Formulation is described in Section 2. The Eq.(73) is rewritten in the fol-

lowing form in the case of a generic layer k:

$$\int_{\Omega_k}\int_{A_k}\Big[\Big((\boldsymbol{D}_p^k+\boldsymbol{A}_p^k)F_s\delta\boldsymbol{u}_s^k\Big)^T\Big(\big(\boldsymbol{Q}_{pp}^k(\boldsymbol{D}_p^k+\boldsymbol{A}_p^k)+\boldsymbol{Q}_{pn}^k(\boldsymbol{D}_{np}^k+\boldsymbol{D}_{nz}^k-\boldsymbol{A}_n^k)\big)F_\tau\boldsymbol{u}_\tau^k-\boldsymbol{\lambda}_p^kF_\tau\theta_\tau^k\Big)+$$
$$\Big((\boldsymbol{D}_{np}^k+\boldsymbol{D}_{nz}^k-\boldsymbol{A}_n^k)F_s\delta\boldsymbol{u}_s^k\Big)^T\Big(\big(\boldsymbol{Q}_{np}^k(\boldsymbol{D}_p^k+\boldsymbol{A}_p^k)+\boldsymbol{Q}_{nn}^k(\boldsymbol{D}_{np}^k+\boldsymbol{D}_{nz}^k-\boldsymbol{A}_n^k)\big)F_\tau\boldsymbol{u}_\tau^k-\boldsymbol{\lambda}_n^kF_\tau\theta_\tau^k\Big)+$$
$$\Big(\boldsymbol{D}_{tp}^kF_s\delta\theta_s^k\Big)^T\Big(\big(\boldsymbol{\kappa}_{pp}^k(-\boldsymbol{D}_{tp}^k)+\boldsymbol{\kappa}_{np}^k(-\boldsymbol{D}_{tn}^k)\big)F_\tau\theta_\tau^k\Big)$$
$$+\Big(\boldsymbol{D}_{tn}^kF_s\delta\theta_s^k\Big)^T\Big(\big(\boldsymbol{\kappa}_{np}^k(-\boldsymbol{D}_{tp}^k)+\boldsymbol{\kappa}_{pp}^k(-\boldsymbol{D}_{tn}^k)\big)F_\tau\theta_\tau^k\Big)\Big]d\Omega_k\,dz=\delta L_e^k. \tag{78}$$

Integrating by parts the Eq.(78), as suggested in Carrera (2002) and Brischetto (2009), the fundamental nuclei are:

$$\boldsymbol{K}_{uu}^{k\tau s}=\int_{A_k}\Big[\Big(-\boldsymbol{D}_p^k+\boldsymbol{A}_p^k\Big)^T\Big(\boldsymbol{Q}_{pp}^k(\boldsymbol{D}_p^k+\boldsymbol{A}_p^k)+\boldsymbol{Q}_{pn}^k(\boldsymbol{D}_{np}^k+\boldsymbol{D}_{nz}^k-\boldsymbol{A}_n^k)\Big)+$$
$$\Big(-\boldsymbol{D}_{np}^k+\boldsymbol{D}_{nz}^k-\boldsymbol{A}_n^k\Big)^T+\Big(\boldsymbol{Q}_{np}^k(\boldsymbol{D}_p^k+\boldsymbol{A}_p^k)+\boldsymbol{Q}_{nn}^k(\boldsymbol{D}_{np}^k+\boldsymbol{D}_{nz}^k-\boldsymbol{A}_n^k)\Big)\Big]F_sF_\tau H_\alpha^kH_\beta^kdz\,, \tag{79}$$

$$\boldsymbol{K}_{u\theta}^{k\tau s}=\int_{A_k}\Big[\Big(-\boldsymbol{D}_p^k+\boldsymbol{A}_p^k\Big)^T\Big(-\boldsymbol{\lambda}_p^k\Big)+\Big(-\boldsymbol{D}_{np}^k+\boldsymbol{D}_{nz}^k-\boldsymbol{A}_n^k\Big)^T\Big(-\boldsymbol{\lambda}_n^k\Big)\Big]F_sF_\tau H_\alpha^kH_\beta^kdz\,, \tag{80}$$

$$\boldsymbol{K}_{\theta u}^{k\tau s}=0 \tag{81}$$

$$\boldsymbol{K}_{\theta\theta}^{k\tau s}=\int_{A_k}\Big[\boldsymbol{D}_{tp}^{kT}\boldsymbol{\kappa}_{pp}^k\boldsymbol{D}_{tp}^k+\boldsymbol{D}_{tp}^{kT}\boldsymbol{\kappa}_{pn}^k\boldsymbol{D}_{tn}^k-\boldsymbol{D}_{tn}^{kT}\boldsymbol{\kappa}_{np}^k\boldsymbol{D}_{tp}^k-\boldsymbol{D}_{tn}^{kT}\boldsymbol{\kappa}_{nn}^k\boldsymbol{D}_{tn}^k\Big]F_sF_\tau H_\alpha^kH_\beta^kdz\,. \tag{82}$$

The fundamental nuclei $\boldsymbol{K}_{uu}^{k\tau s}$ and $\boldsymbol{K}_{u\theta}^{k\tau s}$ are the same obtained in Section 5.1 for the partially coupled problem. The nuclei for boundary conditions on the edge Γ_k are:

$$\boldsymbol{\Pi}_{uu}^{k\tau s}=\int_{A_k}\Big[\boldsymbol{I}_p^{kT}\Big(\boldsymbol{Q}_{pp}^k(\boldsymbol{D}_p^k+\boldsymbol{A}_p^k)+\boldsymbol{Q}_{pn}^k(\boldsymbol{D}_{np}^k+\boldsymbol{D}_{nz}^k-\boldsymbol{A}_n^k)\Big)+\boldsymbol{I}_{np}^{kT}\Big(\boldsymbol{Q}_{np}^k(\boldsymbol{D}_p^k+\boldsymbol{A}_p^k)+$$
$$\boldsymbol{Q}_{nn}^k(\boldsymbol{D}_{np}^k+\boldsymbol{D}_{nz}^k-\boldsymbol{A}_n^k)\Big)\Big]F_sF_\tau H_\alpha^kH_\beta^kdz\,, \tag{83}$$

$$\boldsymbol{\Pi}_{u\theta}^{k\tau s}=\int_{A_k}\Big[\boldsymbol{I}_p^{kT}\Big(-\boldsymbol{\lambda}_p^k\Big)+\boldsymbol{I}_{np}^{kT}\Big(-\boldsymbol{\lambda}_n^k\Big)\Big]F_sF_\tau H_\alpha^kH_\beta^kdz\,, \tag{84}$$

$$\boldsymbol{\Pi}_{\theta u}^{k\tau s}=0 \tag{85}$$

$$\boldsymbol{\Pi}_{\theta\theta}^{k\tau s}=\int_{A_k}\Big[\boldsymbol{I}_{tp}^{kT}\boldsymbol{\kappa}_{pp}^k(-\boldsymbol{D}_{tp}^k)+\boldsymbol{I}_{tp}^{kT}\boldsymbol{\kappa}_{pn}^k(-\boldsymbol{D}_{tn}^k)\Big]F_sF_\tau H_\alpha^kH_\beta^kdz\,. \tag{86}$$

The fundamental nuclei $\mathbf{\Pi}_{uu}^{k\tau s}$ and $\mathbf{\Pi}_{u\theta}^{k\tau s}$ are the same obtained in Section 5.1 for the partially coupled problem. $\boldsymbol{I}_{np}^{k}$ (2×1) and $\boldsymbol{I}_{tp}^{k}$ (1×1) are matrices, to perform the integration by parts, obtained from $\boldsymbol{D}_{np}^{k}$ and $\boldsymbol{D}_{tp}^{k}$ simply replacing the differential operators with 1. Nuclei, given in Eqs.(79)-(82), are introduced in the governing equations (71) in the case of applied temperature on the shell surfaces. In this case, in Eq.(71) the inertial contribute and the mechanical load are discarded. The sovratemperature is directly imposed in the vector θ_{τ}^{k}; therefore, the thermal load $\boldsymbol{p}_{\theta s}^{k}$ is not considered.

5.2.2 Mechanical load and free vibration analysis

In the case of mechanical load applied on the structure or free vibration analysis, in the Eq.(70) the terms $\delta\boldsymbol{\vartheta}_{pG}^{k\,T}\boldsymbol{h}_{pC}^{k}$ and $\delta\boldsymbol{\vartheta}_{nG}^{k\,T}\boldsymbol{h}_{nC}^{k}$ are not considered because it does not exist a gradient of temperature variation. Therefore, the variational statement is:

$$\sum_{k=1}^{N_l}\int_{\Omega_k}\int_{A_k}\left\{\delta\boldsymbol{\varepsilon}_{pG}^{k\,T}\boldsymbol{\sigma}_{pC}^{k}+\delta\boldsymbol{\varepsilon}_{nG}^{k\,T}\boldsymbol{\sigma}_{nC}^{k}-\delta\theta^{k}\eta_{C}^{k}\right\}d\Omega_k dz=\sum_{k=1}^{N_l}\delta L_{e}^{k}-\sum_{k=1}^{N_l}\delta L_{in}^{k}\,. \tag{87}$$

By considering the constitutive equations as obtained in Eqs.(44)-(48), simply discarding the heat fluxes $\boldsymbol{h}_{pC}^{k}$ and $\boldsymbol{h}_{nC}^{k}$:

$$\boldsymbol{\sigma}_{pC}^{k}=\boldsymbol{Q}_{pp}^{k}\boldsymbol{\varepsilon}_{pG}^{k}+\boldsymbol{Q}_{pn}^{k}\boldsymbol{\varepsilon}_{nG}^{k}-\boldsymbol{\lambda}_{p}^{k}\theta^{k}\,, \tag{88}$$

$$\boldsymbol{\sigma}_{nC}^{k}=\boldsymbol{Q}_{np}^{k}\boldsymbol{\varepsilon}_{pG}^{k}+\boldsymbol{Q}_{nn}^{k}\boldsymbol{\varepsilon}_{nG}^{k}-\boldsymbol{\lambda}_{n}^{k}\theta^{k}\,, \tag{89}$$

$$\eta_{C}^{k}=\boldsymbol{\lambda}_{p}^{kT}\boldsymbol{\varepsilon}_{pG}^{k}+\boldsymbol{\lambda}_{n}^{kT}\boldsymbol{\varepsilon}_{nG}^{k}+\chi^{k}\theta^{k}\,. \tag{90}$$

The geometrical relations for shells have been obtained in Section 3, Carrera's Unified Formulation has been described in Section 2. The Eq.(87) is rewritten in the following form for a generic layer k:

$$\begin{aligned}&\int_{\Omega_k}\int_{A_k}\Big[\Big((\boldsymbol{D}_{p}^{k}+\boldsymbol{A}_{p}^{k})F_s\delta\boldsymbol{u}_{s}^{k}\Big)^{T}\Big(\big(\boldsymbol{Q}_{pp}^{k}(\boldsymbol{D}_{p}^{k}+\boldsymbol{A}_{p}^{k})+\boldsymbol{Q}_{pn}^{k}(\boldsymbol{D}_{np}^{k}+\boldsymbol{D}_{nz}^{k}-\boldsymbol{A}_{n}^{k})\big)F_\tau\boldsymbol{u}_{\tau}^{k}-\boldsymbol{\lambda}_{p}^{k}F_\tau\theta_{\tau}^{k}\Big)+\\&\Big((\boldsymbol{D}_{np}^{k}+\boldsymbol{D}_{nz}^{k}-\boldsymbol{A}_{n}^{k})F_s\delta\boldsymbol{u}_{s}^{k}\Big)^{T}\Big(\big(\boldsymbol{Q}_{np}^{k}(\boldsymbol{D}_{p}^{k}+\boldsymbol{A}_{p}^{k})+\boldsymbol{Q}_{nn}^{k}(\boldsymbol{D}_{np}^{k}+\boldsymbol{D}_{nz}^{k}-\boldsymbol{A}_{n}^{k})\big)F_\tau\boldsymbol{u}_{\tau}^{k}-\boldsymbol{\lambda}_{n}^{k}F_\tau\theta_{\tau}^{k}\Big)-\\&F_s\delta\theta_{s}^{kT}\Big(\big(\boldsymbol{\lambda}_{p}^{kT}(\boldsymbol{D}_{p}^{k}+\boldsymbol{A}_{p}^{k})+\boldsymbol{\lambda}_{n}^{kT}(\boldsymbol{D}_{np}^{k}+\boldsymbol{D}_{nz}^{k}-\boldsymbol{A}_{n}^{k})\big)F_\tau\boldsymbol{u}_{\tau}^{k}+\chi^{k}F_\tau\theta_{\tau}^{k}\Big)\Big]\,d\Omega_k\,dz=\delta L_{e}^{k}-\delta L_{in}^{k}\,.\end{aligned} \tag{91}$$

Integrating by parts the Eq.(91), as suggested in Carrera (2002) and Brischetto (2009), the fundamental nuclei $\boldsymbol{K}_{uu}^{k\tau s}$ and $\boldsymbol{K}_{u\theta}^{k\tau s}$ are the same of PVD in Sections 5.1

and 5.2.1, while nuclei $\boldsymbol{K}_{\theta u}^{k\tau s}$ and $\boldsymbol{K}_{\theta\theta}^{k\tau s}$ are:

$$\boldsymbol{K}_{\theta u}^{k\tau s} = \int_{A_k} \Big[-\boldsymbol{\lambda}_p^{kT}(\boldsymbol{D}_p^k + \boldsymbol{A}_p^k) - \boldsymbol{\lambda}_n^{kT}(\boldsymbol{D}_{np}^k + \boldsymbol{D}_{nz}^k - \boldsymbol{A}_n^k) \Big] F_s F_\tau H_\alpha^k H_\beta^k dz \,, \tag{92}$$

$$\boldsymbol{K}_{\theta\theta}^{k\tau sr} = \int_{A_k} \Big[-\boldsymbol{\chi}^k \Big] F_s F_\tau H_\alpha^k H_\beta^k dz \,. \tag{93}$$

Nuclei for boundary conditions on the edge Γ_k, $\boldsymbol{\Pi}_{uu}^{k\tau s}$ and $\boldsymbol{\Pi}_{u\theta}^{k\tau s}$, are the same of PVD in Sections 5.1 and 5.2.1, while the other two state:

$$\boldsymbol{\Pi}_{\theta u}^{k\tau s} = \boldsymbol{\Pi}_{\theta\theta}^{k\tau s} = 0 \,. \tag{94}$$

Nuclei, here obtained, are introduced in the governing equations (71) in the case of applied mechanical load on the shell surfaces or free vibration analysis. In this case, in Eq.(71) the thermal load is discarded. Fundamental nucleus for the inertial contribute is the same already obtained in Eq.(60) of Section 5.1.

6 Navier solution and assembling procedure

In order to write the explicit form of fundamental nuclei obtained in Sections 5.1 and 5.2, the following integrals in the z-thickness direction must be defined:

$$\begin{aligned}
(J^{k\tau s}, J_\alpha^{k\tau s}, J_\beta^{k\tau s}, J_{\frac{\alpha}{\beta}}^{k\tau s}, J_{\frac{\beta}{\alpha}}^{k\tau s}, J_{\alpha\beta}^{k\tau s}) &= \int_{A_k} F_\tau F_s \Big(1, H_\alpha^k, H_\beta^k, \frac{H_\alpha^k}{H_\beta^k}, \frac{H_\beta^k}{H_\alpha^k}, H_\alpha^k H_\beta^k\Big) dz \,, \\
(J^{k\tau_z s}, J_\alpha^{k\tau_z s}, J_\beta^{k\tau_z s}, J_{\frac{\alpha}{\beta}}^{k\tau_z s}, J_{\frac{\beta}{\alpha}}^{k\tau_z s}, J_{\alpha\beta}^{k\tau_z s}) &= \int_{A_k} \frac{\partial F_\tau}{\partial z} F_s \Big(1, H_\alpha^k, H_\beta^k, \frac{H_\alpha^k}{H_\beta^k}, \frac{H_\beta^k}{H_\alpha^k}, H_\alpha^k H_\beta^k\Big) dz \,,
\end{aligned} \tag{95}$$

$$\begin{aligned}
(J^{k\tau s_z}, J_\alpha^{k\tau s_z}, J_\beta^{k\tau s_z}, J_{\frac{\alpha}{\beta}}^{k\tau s_z}, J_{\frac{\beta}{\alpha}}^{k\tau s_z}, J_{\alpha\beta}^{k\tau s_z}) &= \int_{A_k} F_\tau \frac{\partial F_s}{\partial z} \Big(1, H_\alpha^k, H_\beta^k, \frac{H_\alpha^k}{H_\beta^k}, \frac{H_\beta^k}{H_\alpha^k}, H_\alpha^k H_\beta^k\Big) dz \,, \\
(J^{k\tau_z s_z}, J_\alpha^{k\tau_z s_z}, J_\beta^{k\tau_z s_z}, J_{\frac{\alpha}{\beta}}^{k\tau_z s_z}, J_{\frac{\beta}{\alpha}}^{k\tau_z s_z}, J_{\alpha\beta}^{k\tau_z s_z}) &= \int_{A_k} \frac{\partial F_\tau}{\partial z} \frac{\partial F_s}{\partial z} \Big(1, H_\alpha^k, H_\beta^k, \frac{H_\alpha^k}{H_\beta^k}, \frac{H_\beta^k}{H_\alpha^k}, H_\alpha^k H_\beta^k\Big) dz \,.
\end{aligned}$$

By using the Eqs.(95) and developing the matrices products, the explicit forms of fundamental nuclei are obtained.

Navier-type closed form solution is obtained via substitution of harmonic expressions for the displacements and temperature as well as considering the following

material coefficients equal zero: $Q_{16}=Q_{26}=Q_{36}=Q_{45}=0$ and $\lambda_6=\kappa_{12}=0$. The following harmonic assumptions can be made for the variables, which correspond to simply supported boundary conditions:

$$\begin{aligned}
u_\tau^k &= \sum_{m,n}(\hat{U}_\tau^k)\cos\left(\frac{m\pi\alpha_k}{a_k}\right)\sin\left(\frac{n\pi\beta_k}{b_k}\right), \qquad k=1,N_l\,,\\
v_\tau^k &= \sum_{m,n}(\hat{V}_\tau^k)\sin\left(\frac{m\pi\alpha_k}{a_k}\right)\cos\left(\frac{n\pi\beta_k}{b_k}\right), \qquad \tau=t,b,r\,,\\
(w_\tau^k,\theta_\tau^k) &= \sum_{m,n}(\hat{W}_\tau^k,\hat{\theta}_\tau^k)\sin\left(\frac{m\pi\alpha_k}{a_k}\right)\sin\left(\frac{n\pi\beta_k}{b_k}\right), \qquad r=2,N\,,
\end{aligned} \tag{96}$$

where $\hat{U}_\tau^k$, $\hat{V}_\tau^k$, $\hat{W}_\tau^k$, $\hat{\theta}_\tau^k$ are the amplitudes.

Fundamental nucleus $\boldsymbol{K}_{uu}^{k\tau s}$, of dimension (3×3), is in common for each considered case:

$$\begin{aligned}
K_{uu_{11}} &= Q_{55}^k J_{\alpha\beta}^{k\tau_z s_z} + \frac{1}{R_\alpha^k}Q_{55}^k(-J_\beta^{k\tau_z s} - J_\beta^{k\tau s_z} + \frac{1}{R_\alpha^k}J_{\beta/\alpha}^{k\tau s}) + Q_{11}^k J_{\beta/\alpha}^{k\tau s}\bar{\alpha}^2 + Q_{66}^k J_{\alpha/\beta}^{k\tau s}\bar{\beta}^2\,,\\
K_{uu_{12}} &= J^{k\tau s}\bar{\alpha}\bar{\beta}(Q_{12}^k+Q_{66}^k) = K_{uu_{21}}\,,\\
K_{uu_{13}} &= Q_{55}^k(J_\beta^{k\tau_z s}\bar{\alpha} - \frac{1}{R_\alpha^k}J_{\beta/\alpha}^{k\tau s}\bar{\alpha}) - Q_{13}^k J_\beta^{k\tau s_z}\bar{\alpha} - \frac{1}{R_\alpha^k}Q_{11}^k J_{\beta/\alpha}^{k\tau s}\bar{\alpha} - Q_{12}^k J^{k\tau s}\bar{\alpha}\frac{1}{R_\beta^k}\,,\\
K_{uu_{22}} &= Q_{44}^k J_{\alpha\beta}^{k\tau_z s_z} + \frac{1}{R_\beta^k}Q_{44}^k(-J_\alpha^{k\tau_z s} - J_\alpha^{k\tau s_z} + \frac{1}{R_\beta^k}J_{\alpha/\beta}^{k\tau s}) + Q_{22}^k J_{\alpha/\beta}^{k\tau s}\bar{\beta}^2 + Q_{66}^k J_{\beta/\alpha}^{k\tau s}\bar{\alpha}^2\,,\\
K_{uu_{23}} &= Q_{44}^k(J_\alpha^{k\tau_z s}\bar{\beta} - \frac{1}{R_\beta^k}J_{\alpha/\beta}^{k\tau s}\bar{\beta}) - Q_{23}^k J_\alpha^{k\tau s_z}\bar{\beta} - \frac{1}{R_\beta^k}Q_{22}^k J_{\alpha/\beta}^{k\tau s}\bar{\beta} - \frac{1}{R_\alpha^k}Q_{12}^k J^{k\tau s}\bar{\beta}\,,\\
K_{uu_{31}} &= Q_{55}^k J_\beta^{k\tau s_z}\bar{\alpha} - Q_{55}^k\frac{1}{R_\alpha^k}J_{\beta/\alpha}^{k\tau s}\bar{\alpha} - Q_{13}^k J_\beta^{k\tau_z s}\bar{\alpha} - \frac{1}{R_\alpha^k}Q_{11}^k J_{\beta/\alpha}^{k\tau s}\bar{\alpha} - \frac{1}{R_\beta^k}Q_{12}^k J^{k\tau s}\bar{\alpha}\,,\\
K_{uu_{32}} &= Q_{44}^k(J_\alpha^{k\tau s_z}\bar{\beta} - \frac{1}{R_\beta^k}J_{\alpha/\beta}^{k\tau s}\bar{\beta}) - Q_{23}^k J_\alpha^{k\tau_z s}\bar{\beta} - \frac{1}{R_\beta^k}Q_{22}^k J_{\alpha/\beta}^{k\tau s}\bar{\beta} - \frac{1}{R_\alpha^k}Q_{12}^k J^{k\tau s}\bar{\beta}\,,\\
K_{uu_{33}} &= Q_{55}^k J_{\beta/\alpha}^{k\tau s}\bar{\alpha}^2 + Q_{44}^k J_{\alpha/\beta}^{k\tau s}\bar{\beta}^2 + Q_{33}^k J_{\alpha\beta}^{k\tau_z s_z} + \frac{1}{R_\alpha^k}(\frac{1}{R_\alpha^k}Q_{11}^k J_{\beta/\alpha}^{k\tau s} + Q_{13}^k J_\beta^{k\tau s_z}\\
&\quad + Q_{13}^k J_\beta^{k\tau_z s}) + \frac{2}{R_\alpha^k R_\beta^k}J^{k\tau s}Q_{12}^k + \frac{1}{R_\beta^k}(\frac{1}{R_\beta^k}Q_{22}^k J_{\alpha/\beta}^{k\tau s} + Q_{23}^k J_\alpha^{k\tau_z s} + Q_{23}^k J_\alpha^{k\tau s_z})\,.
\end{aligned} \tag{97}$$

Fundamental nucleus $\boldsymbol{K}_{u\theta}^{k\tau s}$, of dimension (3×1), is in common for the partially

coupled case and for each extension of the fully coupled case:

$$K_{u\theta_{11}} = \bar{\alpha} J_{\beta}^{k\tau s} \lambda_1^k , \quad K_{u\theta_{21}} = \bar{\beta} J_{\alpha}^{k\tau s} \lambda_2^k , \quad K_{u\theta_{31}} = -\frac{1}{R_{\alpha}^k} J_{\beta}^{k\tau s} \lambda_1^k - \frac{1}{R_{\beta}^k} J_{\alpha}^{k\tau s} \lambda_2^k - J_{\alpha\beta}^{k\tau_z s} \lambda_3^k . \tag{98}$$

Fundamental nuclei $\boldsymbol{K}_{\theta u}^{k\tau s}$, of dimension (1×3), and $\boldsymbol{K}_{\theta\theta}^{k\tau s}$, of dimension (1×1), for the fully coupled thermo-mechanical analysis, in the case of applied temperature on the surfaces, are:

$$K_{\theta u_{11}} = K_{\theta u_{12}} = K_{\theta u_{13}} = 0 , \tag{99}$$

$$K_{\theta\theta_{11}} = -J_{\substack{\beta \\ \alpha}}^{k\tau s} \bar{\alpha}^2 \kappa_{11} - J_{\substack{\alpha \\ \beta}}^{k\tau s} \bar{\beta}^2 \kappa_{22} - J_{\alpha\beta}^{k\tau_z s_z} \kappa_{33} . \tag{100}$$

Fundamental nuclei $\boldsymbol{K}_{\theta u}^{k\tau s}$, of dimension (1×3), and $\boldsymbol{K}_{\theta\theta}^{k\tau s}$, of dimension (1×1), for the fully coupled thermo-mechanical analysis, in the case of applied mechanical load and free vibration problem, are:

$$K_{\theta u_{11}} = \bar{\alpha} J_{\beta}^{k\tau s} \lambda_1^k , \qquad K_{\theta u_{12}} = \bar{\beta} J_{\alpha}^{k\tau s} \lambda_2^k , \qquad K_{\theta u_{13}} = -\frac{1}{R_{\alpha}^k} J_{\beta}^{k\tau s} \lambda_1^k - \frac{1}{R_{\beta}^k} J_{\alpha}^{k\tau s} \lambda_2^k - J_{\alpha\beta}^{k\tau_z s} \lambda_3^k , \tag{101}$$

$$K_{\theta\theta_{11}} = -J_{\alpha\beta}^{k\tau s} \chi . \tag{102}$$

The fundamental nucleus of the inertial matrix $\boldsymbol{M}_{uu}^{k\tau s}$, of dimension (3×3), is:

$$\begin{aligned} M_{uu_{11}} &= \rho^k J_{\alpha\beta}^{k\tau s} , \quad M_{uu_{12}} = M_{uu_{13}} = 0 , \quad M_{uu_{21}} = 0 , \quad M_{uu_{22}} = \rho^k J_{\alpha\beta}^{k\tau s} , \quad M_{uu_{23}} = 0 , \\ M_{uu_{31}} &= M_{uu_{32}} = 0 , \quad M_{uu_{33}} = \rho^k J_{\alpha\beta}^{k\tau s} . \end{aligned} \tag{103}$$

For each fundamental nucleus, $\bar{\alpha} = m\pi/a$ and $\bar{\beta} = n\pi/b$, where m and n are the wave numbers in in-plane directions, and a and b the shell dimensions.

By starting from the fundamental nuclei described in this section, matrices can be obtained for the considered multilayered shells by simply expanding and assembling via the indexes k, τ, s. By expanding via indexes τ, s, the order of expansion N from 1 to 4 in the thickness direction is considered. The matrices are obtained for each considered layer, and the index k permits the multilayer assembling procedure, which can either be ESL or LW.

6.1 Acronyms

A system of acronyms is here given in order to define the several refined two-dimensional models developed in this work. The choice made in this paper is that displacements can be in ESL or LW form, but the temperature is always considered in LW form. Therefore, a two-dimensional model is defined as ESL or LW, depending on the choice made for the displacement. ESL models are indicated as ED1-ED4, where E means the ESL approach, D means that the Principle of Virtual Displacements or their extensions to thermo-mechanical analysis have been employed; the last digit, from 1 to 4, indicates the order of expansion in the thickness direction for both displacements and temperature. In the case of LW models, the letter E is replaced by a letter L, therefore the relative models are indicated as LD1-LD4. In the case of a thermo-mechanical analysis, additional parenthesis are introduced in the acronyms: (θ_a) is added in the case of partially coupled thermo-mechanical analysis with a linear assumed temperature profile; (θ_c) is used to indicate the case of partially coupled thermo-mechanical analysis with a calculated temperature profile; (TM) means a fully coupled thermo(T)-mechanical(M) analysis. No parenthesis are added in the case of a pure mechanical problem.

7 Results

The results proposed in this section, consider three different cases: - shells with imposed temperature at the two external surfaces; - shells subjected to a mechanical load on top surface; - free vibration analysis of shells. The considered cylindrical shell panels are simply supported (see Figure 2). The radius of curvature in β direction is $R_\beta = \infty$, the radius of curvature in α direction is $R_\alpha = 10\,m$ with angle Φ equals $\frac{\pi}{3}$. The in-plane shell dimensions are $a = \frac{\pi}{3} R_\alpha = 10.47197551\,m$ and $b = 1\,m$. The investigated thickness ratios are $R_\alpha/h = 5, 10, 50, 100$ and 1000, which means total thickness of the shell $h = 2, 1, 0.2, 0.1$ and $0.01\,m$, respectively. Three different layered shells are investigated for each proposed case. The first is a one-layered isotropic shell in $Al2024$ with Young's modulus $E = 73\,GPa$, Poisson's ratio $\nu = 0.3$ and mass density $\rho = 2800\,Kg/m^3$. The thermal properties are the specific heat per unit mass $C_v = 897\,J/Kg\,K$, the thermal expansion coefficient $\alpha = 25 \times 10^{-6}\,1/K$ and the conductivity coefficient $\kappa = 130\,W/mK$. The two-layered isotropic shell has two layers of thickness $h_1 = h_2 = h/2$, the bottom layer is in $Al2024$ and the top layer is in $Ti22$. The mechanical properties of the $Ti22$ layer are $E = 110\,GPa$, $\nu = 0.32$ and $\rho = 4420\,Kg/m^3$. Its thermal properties are $C_v = 560\,J/Kg\,K$, $\alpha = 8.6 \times 10^{-6}\,1/K$ and $\kappa = 21.9\,W/mK$. The third case is a three-layered composite $(0^\circ/90^\circ/0^\circ)$ shell where the three layers have the same thickness $h_1 = h_2 = h_3 = h/3$. The elastic properties of the embedded carbon fi-

bre reinforced layers are Young's longitudinal modulus $E_1 = 172.72\,GPa$, Young's transverse modulus $E_2 = E_3 = 6.909\,GPa$, Poisson's ratio $\nu = 0.25$, shear modulus $G_{12} = G_{13} = 3.45\,GPa$ and $G_{23} = 1.38\,GPa$, mass density $\rho = 1940\,Kg/m^3$. The thermal properties are the specific heat-per-unit mass $C_v = 846\,J/Kg\,K$, longitudinal thermal expansion coefficient $\alpha_1 = 0.57 \times 10^{-6}\,1/K$, transverse thermal expansion coefficients $\alpha_2 = \alpha_3 = 35.6 \times 10^{-6}\,1/K$, longitudinal conductivity coefficient $\kappa_{11} = 36.42\,W/mK$ and transverse conductivity coefficients $\kappa_{22} = \kappa_{33} = 0.96\,W/mK$.

7.1 Imposed temperature on the surfaces

The considered shells have an imposed sovra-temperature at the top $\theta_t = 1.0\,K$ and at the bottom $\theta_b = 0.0\,K$. The temperature is bi-sinusoidal in the in-plane directions with wave numbers $m = n = 1$. The partially coupled models with assumed temperature profile (ED1(θ_a)-ED4(θ_a), LD1(θ_a)-LD4(θ_a), FSDT(θ_a)-CLT(θ_a)), and those with calculated temperature profile (ED1(θ_c)-ED4(θ_c), LD1(θ_c)-LD4(θ_c), FSDT(θ_c)-CLT(θ_c)) have been validated extensively in the authors' previous works [Brischetto and Carrera (2009); Carrera (2000); Carrera (2002); Brischetto (2009); Brischetto et al. (2008); Brischetto and Carrera (2010)]. In the partially coupled models, the temperature profile must be a priori defined: - assuming it linear through the thickness (θ_a) from $\theta_t = 1.0\,K$ to $\theta_b = 0.0\,K$ as shown in Figure 3; - calculating it by solving the Fourier heat conduction equation (θ_c) where the thermal boundary conditions are $\theta_t = 1.0\,K$ at the top $\theta_b = 0.0\,K$ at the bottom. The temperature profile permits the thermal load to be obtained for Eq.(56). In the fully coupled models, the sovra-temperature is directly imposed in the vector θ_τ^k and the displacement and temperature profile are directly obtained by solving the governing relation in Eq.(71).

Tables 1-2 and Figure 4 consider an isotropic one-layered cylindrical shell. ESL and LW theories with orders of expansion $N = 1 \div 4$ are coincident because the considered shell has only one layer. Table 1 gives the transverse displacement w in the middle of the shell, Table 2 gives the in-plane displacement u at the top of the shell. For thick shells the temperature profile is not linear, even when it is isotropic and one-layered, see Figure 4. Thin shells have a linear temperature profile in the thickness direction. For thick shells, displacements obtained with partially coupled models (θ_a) are different from those obtained with partially coupled (θ_c) or fully coupled models (TM) (an error due to the assumption of a linear temperature profile). When the shell is thin, the three models are coincident because the temperature profile is linear, as indicated in the Figure 4. Classical theories, such as CLT and FSDT, give very large errors for each proposed model (θ_a, θ_c and TM), even when the shell is thin: their degrees of freedom are not sufficient to exhaustively

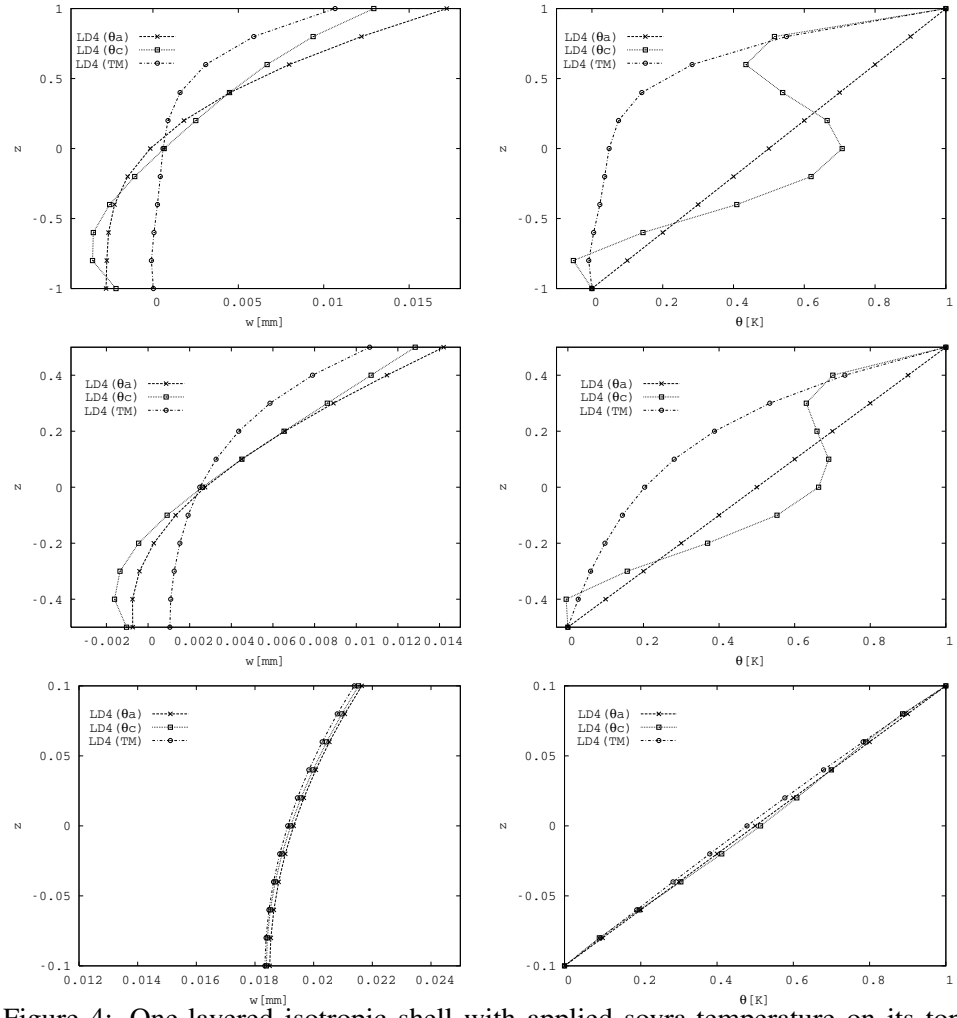

Figure 4: One-layered isotropic shell with applied sovra-temperature on its top and bottom surfaces. Displacement w and sovra-temperature θ vs. z for $R_\alpha/h = 5, 10, 50$ (top, middle and bottom figures, respectively).

Table 1: One-layered isotropic shell with applied sovra-temperature on its top and bottom surfaces. Displacement w in $[mm]$ for several two-dimensional theories and thickness ratios.

	R_α/h	5	10	50	100	1000
LD4(θ_a)	$w(0)$	-0.0002	0.0027	0.0193	0.0419	0.1431
LD4(θ_c)	$w(0)$	0.0007	0.0026	0.0192	0.0418	0.1431
LD4(TM)	$w(0)$	0.0006	0.0025	0.0191	0.0417	0.1431
LD2(θ_a)	$w(0)$	-0.0003	0.0024	0.0192	0.0418	0.1431
LD2(θ_c)	$w(0)$	-0.0004	0.0023	0.0191	0.0417	0.1431
LD2(TM)	$w(0)$	-0.0004	0.0023	0.0191	0.0417	0.1431
FSDT(θ_a)	$w(0)$	0.0028	0.0052	0.0273	0.0589	0.2009
FSDT(θ_c)	$w(0)$	0.0028	0.0052	0.0273	0.0589	0.2009
FSDT(TM)	$w(0)$	0.0028	0.0052	0.0273	0.0589	0.2009
CLT(θ_a)	$w(0)$	0.0023	0.0048	0.0270	0.0586	0.2009
CLT(θ_c)	$w(0)$	0.0023	0.0048	0.0270	0.0586	0.2009
CLT(TM)	$w(0)$	0.0023	0.0048	0.0270	0.0586	0.2009

model the thermal part. LD2 theory gives good results for thin and moderately thin shells ($R_\alpha/h = 50, 100, 1000$). The partially coupled models with calculated temperature profiles (θ_c) and the fully coupled models (TM) are almost coincident, but the solution of Fourier's heat conduction equation is difficult for thick shells ($R_\alpha/h = 5, 10$, as illustrated in Figure 4 for the transverse displacement w and the sovra-temperature profile θ, and in Table 2 for the in-plane displacement u). FSDT and CLT theories always give the same results because the temperature profile is linear for θ_a, θ_c and TM models. In conclusion, the fully coupled models are a valid alternative to partially coupled models with calculated temperature profile θ_c: they give the same results, but in a simpler way (without solving the Fourier equation, but directly obtaining both displacements and temperature from the governing equation).

A two-layered isotropic shell is investigated in Tables 3 and 4, and in Figure 5. The partially coupled models, with assumed temperature profile (θ_a), give large errors for both thick and thin shells: as suggested in Figure 5, the temperature profile is never linear, even when the shell is thin; in fact, the two layers have different conductivity coefficients and this means linear temperature profiles in each layer but with different slopes. As in the one-layered case, partially coupled models with

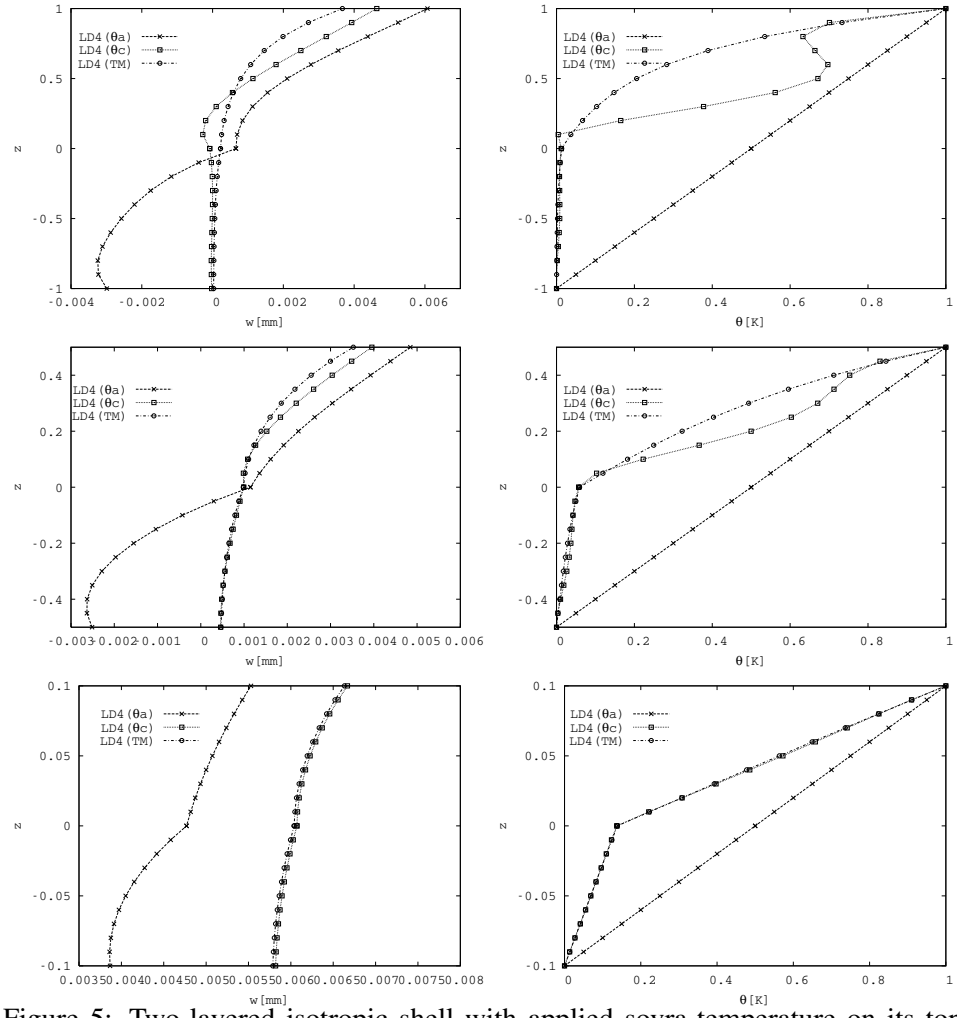

Figure 5: Two-layered isotropic shell with applied sovra-temperature on its top and bottom surfaces. Displacement w and sovra-temperature θ vs. z for $R_\alpha/h = 5, 10, 50$ (top, middle and bottom figures, respectively).

Table 2: One-layered isotropic shell with applied sovra-temperature on its top and bottom surfaces. Displacement u in $[10^{-4}m]$ for several two-dimensional theories and thickness ratios.

	R_α/h	5	10	50	100	1000
LD4(θ_a)	$u(h/2)$	-0.0145	-0.0127	-0.0095	-0.0083	0.0028
LD4(θ_c)	$u(h/2)$	-0.0111	-0.0116	-0.0095	-0.0083	0.0028
LD4(TM)	$u(h/2)$	-0.0091	-0.0094	-0.0093	-0.0083	0.0028
LD2(θ_a)	$u(h/2)$	-0.0123	-0.0118	-0.0095	-0.0083	0.0028
LD2(θ_c)	$u(h/2)$	-0.0107	-0.0099	-0.0093	-0.0082	0.0028
LD2(TM)	$u(h/2)$	-0.0105	-0.0099	-0.0093	-0.0082	0.0028
FSDT(θ_a)	$u(h/2)$	-0.0131	-0.0136	-0.0131	-0.0116	0.0040
FSDT(θ_c)	$u(h/2)$	-0.0131	-0.0136	-0.0131	-0.0116	0.0040
FSDT(TM)	$u(h/2)$	-0.0131	-0.0136	-0.0131	-0.0116	0.0040
CLT(θ_a)	$u(h/2)$	-0.0141	-0.0139	-0.0131	-0.0116	0.0040
CLT(θ_c)	$u(h/2)$	-0.0141	-0.0139	-0.0131	-0.0116	0.0040
CLT(TM)	$u(h/2)$	-0.0141	-0.0139	-0.0131	-0.0116	0.0040

a calculated temperature profile (θ_c) and fully coupled models are almost coincident, but the solution of Fourier's heat conduction equation is difficult for thick shells ($R_\alpha/h = 5, 10$) as shown in Figure 5. The shell is two-layered with a strong transverse anisotropy, therefore the importance of the kinematics for the displacements approximation can clearly be noticed in Tables 3 and 4 and in Figure 5: refined theories are preferred to classical theories, such as CLT and FSDT, which are inadequate for each proposed thermo-mechanical model. LD4, ED4 and ED2 kinematics are coincident for $R_\alpha/h = 50, 100, 1000$.

Transverse displacement w in the middle of the three-layered composite shell, and in-plane displacement u at its top are given in Tables 5 and 6, respectively. Figure 6 shows transverse displacement and sovra-temperature in the thickness direction z for thick and thin shells. The three layers are made of the same material (carbon fibre reinforced layers), the only difference is the fibre orientation (0° for the bottom and top layer, and 90° for the middle layer). This means that that the conductivity coefficient κ_{33} is the same for the three layers, but the in-plane coefficients κ_{11} and κ_{22} are exchanged in the layers (the in-plane dimensions a and b are not the same). Therefore, the temperature profiles in Figure 6 are easily explained: the profile is not linear even when the shell is thin. Figure 6 explains the results in Tables

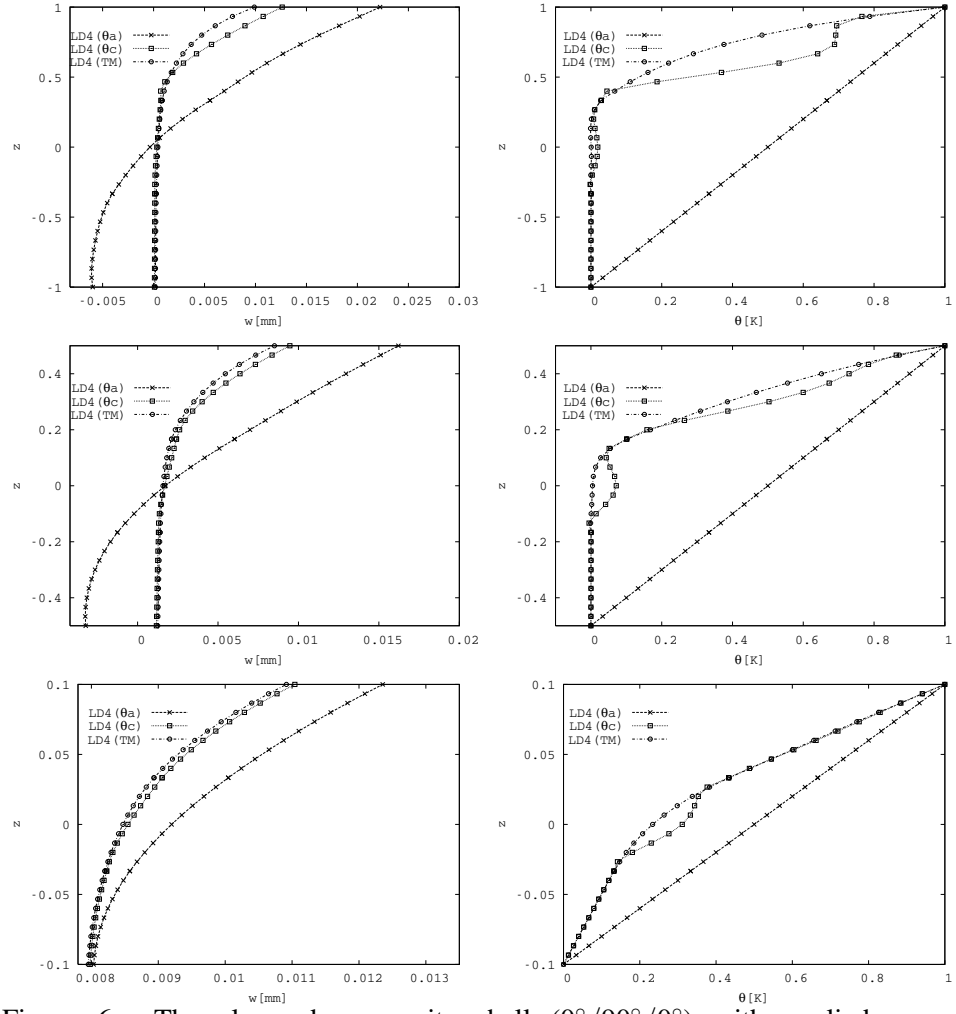

Figure 6: Three-layered composite shell $(0°/90°/0°)$ with applied sovra-temperature on its top and bottom surfaces. Displacement w and sovra-temperature θ vs. z for $R_\alpha/h = 5, 10, 50$ (top, middle and bottom figures, respectively).

Table 3: Two-layered isotropic shell with applied sovra-temperature on its top and bottom surfaces. Displacement w in [mm] for several two-dimensional theories and thickness ratios.

	R_α/h	5	10	50	100	1000
LD4(θ_a)	$w(0)$	0.0007	0.0011	0.0048	0.0117	0.0634
LD4(θ_c)	$w(0)$	-0.0001	0.0010	0.0061	0.0129	0.0424
LD4(TM)	$w(0)$	0.0002	0.0010	0.0060	0.0129	0.0424
ED4(θ_a)	$w(0)$	-0.0001	0.0007	0.0047	0.0116	0.0634
ED4(T_c)	$w(0)$	-0.0003	0.0009	0.0060	0.0129	0.0424
ED4(TM)	$w(0)$	0.0002	0.0009	0.0060	0.0129	0.0424
LD2(θ_a)	$w(0)$	0.0006	0.0011	0.0048	0.0117	0.0634
LD2(θ_c)	$w(0)$	0.0003	0.0010	0.0060	0.0129	0.0424
LD2(TM)	$w(0)$	0.0003	0.0010	0.0060	0.0129	0.0424
FSDT(θ_a)	$w(0)$	0.0007	0.0012	0.0069	0.0172	0.0916
FSDT(θ_c)	$w(0)$	0.0010	0.0018	0.0089	0.0189	0.0616
FSDT(TM)	$w(0)$	0.0010	0.0018	0.0089	0.0189	0.0617
CLT(θ_a)	$w(0)$	0.0004	0.0010	0.0067	0.0170	0.0916
CLT(θ_c)	$w(0)$	0.0009	0.0017	0.0088	0.0188	0.0617
CLT(TM)	$w(0)$	0.0009	0.0017	0.0088	0.0188	0.0617

5 and 6: for thin and moderately thin shells θ_c and TM models give the same results, for thick shells there are some differences because the solution of Fourier's heat conduction equation is difficult for thick shells ($R_\alpha/h = 5, 10$). This fact is confirmed by the in-plane displacement u for $R_\alpha/h = 5, 10, 50$ in Table 6. LD4(θ_a) theory is correct for very thin shells ($R_\alpha/h = 1000$). The transverse anisotropy, in terms of elastic properties, remarks the importance of higher orders of expansion for the displacement and the inadequacy of CLT and FSDT is confirmed.

For all the three proposed cases, the fully coupled models appear to be the best solution: they give the same results as the partially coupled θ_c models, but both the displacements and temperature are directly obtained from the governing equations. On the contrary, in the θ_c model, the temperature profile must be a priori calculated, by solving the Fourier heat conduction equation, and then introduced into the governing equation as an external load.

Table 4: Two-layered isotropic shell with applied sovra-temperature on its top and bottom surfaces. Displacement u in $[10^{-4}m]$ for several two-dimensional theories and thickness ratios.

	R_α/h	5	10	50	100	1000
LD4(θ_a)	$u(h/2)$	-0.0052	-0.0045	-0.0035	-0.0033	0.0010
LD4(θ_c)	$u(h/2)$	-0.0040	-0.0035	-0.0027	-0.0023	0.0009
LD4(TM)	$u(h/2)$	-0.0031	-0.0031	-0.0027	-0.0023	0.0009
ED4(θ_a)	$u(h/2)$	-0.0051	-0.0045	-0.0035	-0.0033	0.0010
ED4(θ_c)	$u(h/2)$	-0.0037	-0.0034	-0.0027	-0.0023	0.0009
ED4(TM)	$u(h/2)$	-0.0031	-0.0031	-0.0027	-0.0023	0.0009
LD2(θ_a)	$u(h/2)$	-0.0047	-0.0045	-0.0035	-0.0033	0.0010
LD2(θ_c)	$u(h/2)$	-0.0033	-0.0031	-0.0027	-0.0023	0.0009
LD2(TM)	$u(h/2)$	-0.0033	-0.0031	-0.0027	-0.0023	0.0009
FSDT(θ_a)	$u(h/2)$	-0.0046	-0.0048	-0.0050	-0.0047	0.0015
FSDT(θ_c)	$u(h/2)$	-0.0036	-0.0038	-0.0038	-0.0033	0.0013
FSDT(TM)	$u(h/2)$	-0.0035	-0.0038	-0.0038	-0.0033	0.0013
CLT(θ_a)	$u(h/2)$	-0.0050	-0.0049	-0.0050	-0.0047	0.0015
CLT(θ_c)	$u(h/2)$	-0.0039	-0.0039	-0.0038	-0.0033	0.0013
CLT(TM)	$u(h/2)$	-0.0038	-0.0039	-0.0038	-0.0033	0.0013

7.2 Applied mechanical load

The considered shells are subjected to a mechanical load applied at the top in the z direction, with amplitude $p_{zt} = -200000\,Pa$ and harmonic distribution in the plane (waves number $m = n = 1$). A comparison is made between the pure mechanical models (see Eq.(56), with inertial contribution and thermal load discarded) and the fully coupled models (TM) (see Eq.(71), with inertial contribution and thermal load discarded). In general, when a model considers the thermo-mechanical coupling, smaller displacements are obtained and a temperature profile in the thickness direction is originated.

The first case considers a one-layered isotropic shell, the correspondent plate case has already analyzed in Brischetto and Carrera (2010) and Carrera et al. (2007). Transverse and in-plane displacements are given for the pure mechanical models and for the fully coupled thermo-mechanical models in Table 7. The pure mechanical models give larger displacements than the fully coupled models; in the

Table 5: Three-layered composite shell $(0°/90°/0°)$ with applied sovra-temperature on its top and bottom surfaces. Displacement w in $[mm]$ for several two-dimensional theories and thickness ratios.

	R_α/h	5	10	50	100	1000
LD4(θ_a)	$w(0)$	-0.0003	0.0017	0.0092	0.0137	0.0101
LD4(θ_c)	$w(0)$	0.0003	0.0017	0.0085	0.0131	0.0100
LD4(TM)	$w(0)$	0.0004	0.0016	0.0085	0.0131	0.0100
ED4(θ_a)	$w(0)$	-0.0003	0.0018	0.0091	0.0136	0.0101
ED4(θ_c)	$w(0)$	0.0001	0.0016	0.0084	0.0131	0.0100
ED4(TM)	$w(0)$	0.0004	0.0016	0.0084	0.0131	0.0100
LD2(θ_a)	$w(0)$	-0.0005	0.0016	0.0091	0.0136	0.0101
LD2(θ_c)	$w(0)$	0.0004	0.0015	0.0084	0.0130	0.0100
LD2(TM)	$w(0)$	0.0004	0.0015	0.0084	0.0131	0.0100
FSDT(θ_a)	$w(0)$	0.0017	0.0029	0.0119	0.0181	0.0139
FSDT(θ_c)	$w(0)$	0.0011	0.0022	0.0110	0.0174	0.0139
FSDT(TM)	$w(0)$	0.0011	0.0021	0.0110	0.0173	0.0139
CLT(θ_a)	$w(0)$	0.0013	0.0026	0.0119	0.0182	0.0139
CLT(θ_c)	$w(0)$	0.0010	0.0021	0.0111	0.0175	0.0139
CLT(TM)	$w(0)$	0.0010	0.0021	0.0111	0.0175	0.0139

latter, the deformation field produces a change in temperature in the considered body. The differences in displacements, as suggested in Nowinski's book [Nowinski (1978)] for a general structure, and then confirmed in Carrera et al. (2007) and in Brischetto and Carrera (2010) for the plate case, is about $0.5\% \div 1\%$ for each thickness ratio and each proposed two-dimensional theory. CLT and FSDT theories properly work only for thin shells ($R_\alpha/h = 1000$) in the case of mechanical model. LD4 and LD4(TM) models are compared in Figure 7, in terms of transverse displacement, for a moderately thin shell. Through the thickness z, the transverse displacement obtained with the pure mechanical model is always larger than that obtained with the fully coupled model. This happens because, when a mechanical load is applied, a small part of the work done by this load, is used to develop an increment in temperature (the maximum value is about $0.01\,K$). The temperature values are remarkably small because of the small coupling effect between the thermal and mechanical fields. The bending problem, as described in Figure 7, leads to an increment in temperature for the compressed part of the shell and a decrease in

Table 6: Three-layered composite shell $(0^\circ/90^\circ/0^\circ)$ with applied sovra-temperature on its top and bottom surfaces. Displacement u in $[10^{-4}m]$ for several two-dimensional theories and thickness ratios.

	R_α/h	5	10	50	100	1000
LD4(θ_a)	$u(h/2)$	0.0049	0.0013	-0.0005	0.0033	0.0021
LD4(θ_c)	$u(h/2)$	0.0025	0.0011	0.0009	0.0036	0.0021
LD4(TM)	$u(h/2)$	0.0016	0.0010	0.0011	0.0037	0.0021
ED4(θ_a)	$u(h/2)$	0.0048	0.0006	-0.0006	0.0032	0.0021
ED4(θ_c)	$u(h/2)$	0.0025	0.0007	0.0008	0.0036	0.0021
ED4(TM)	$u(h/2)$	0.0017	0.0006	0.0009	0.0037	0.0021
LD2(θ_a)	$u(h/2)$	0.0053	0.0012	-0.0005	0.0032	0.0021
LD2(θ_c)	$u(h/2)$	0.0019	0.0009	0.0010	0.0037	0.0021
LD2(TM)	$u(h/2)$	0.0018	0.0009	0.0010	0.0037	0.0021
FSDT(θ_a)	$u(h/2)$	-0.0104	-0.0098	-0.0023	0.0034	0.0026
FSDT(θ_c)	$u(h/2)$	-0.0045	-0.0044	-0.0003	0.0040	0.0026
FSDT(TM)	$u(h/2)$	-0.0043	-0.0040	-0.0001	0.0040	0.0026
CLT(θ_a)	$u(h/2)$	-0.0116	-0.0102	-0.0023	0.0035	0.0026
CLT(θ_c)	$u(h/2)$	-0.0050	-0.0045	-0.0002	0.0041	0.0026
CLT(TM)	$u(h/2)$	-0.0048	-0.0041	0.0000	0.0041	0.0026

temperature for the enlarged part of the shell.

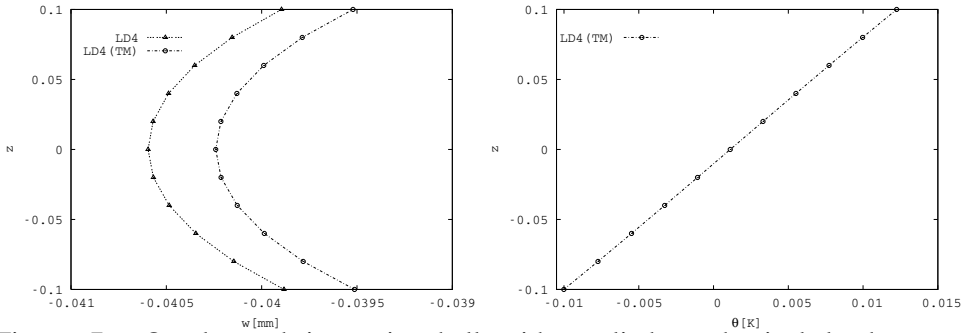

Figure 7: One-layered isotropic shell with applied mechanical load $p_z = -200000\ Pa$ at the top. Displacement w and sovra-temperature θ vs. z for $R_\alpha/h = 50$.

Table 7: One-layered isotropic shell with applied mechanical load $p_z = -200000\ Pa$ at the top. Displacements u and w in $[10^{-6}m]$ for several two-dimensional theories and thickness ratios.

	R_α/h	5	10	50	100	1000
LD4(TM)	$w(0)$	-0.2108	-0.9692	-40.241	-277.03	-25410
LD4	$w(0)$	-0.2117	-0.9740	-40.596	-279.50	-25549
LD4(TM)	$u(h/2)$	0.0272	0.0418	0.7926	2.0995	-137.65
LD4	$u(h/2)$	0.0286	0.0433	0.8020	2.1252	-137.89
LD2(TM)	$w(0)$	-0.2158	-0.8897	-39.757	-276.19	-25410
LD2	$w(0)$	-0.2154	-0.8933	-40.107	-278.66	-25548
LD2(TM)	$u(h/2)$	0.0001	0.0216	0.7813	2.0928	-137.65
LD2	$u(h/2)$	0.0012	0.0230	0.7906	2.1184	-137.89
FSDT(TM)	$w(0)$	-0.4332	-1.0588	-39.832	-274.65	-25277
FSDT	$w(0)$	-0.4340	-1.0647	-40.518	-279.55	-25552
FSDT(TM)	$u(h/2)$	0.0088	0.0378	0.8038	2.0961	-137.41
FSDT	$u(h/2)$	0.0091	0.0386	0.8211	2.1463	-137.90
CLT(TM)	$w(0)$	-0.0408	-0.3109	-36.412	-268.80	-25276
CLT	$w(0)$	-0.0416	-0.3168	-37.100	-273.71	-25551
CLT(TM)	$u(h/2)$	0.0111	0.0428	0.8302	2.1461	-137.40
CLT	$u(h/2)$	0.0113	0.0436	0.8473	2.1960	-137.89

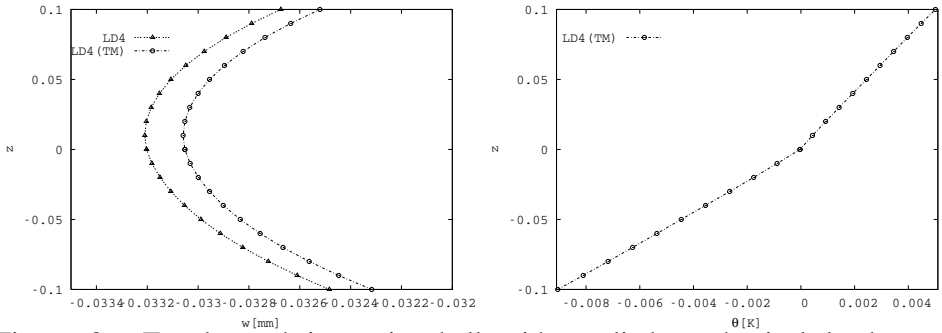

Figure 8: Two-layered isotropic shell with applied mechanical load $p_z = -200000\ Pa$ at the top. Displacement w and sovra-temperature θ vs. z for $R_\alpha/h = 50$.

Table 8: Two-layered isotropic shell with applied mechanical load $p_z = -200000\ Pa$ at the top. Displacements u and w in $[10^{-6}m]$ for several two-dimensional theories and thickness ratios.

	R_α/h	5	10	50	100	1000
LD4(TM)	$w(0)$	-0.1967	-0.8159	-33.052	-226.16	-20294
LD4	$w(0)$	-0.1969	-0.8173	-33.203	-227.09	-20325
LD4(TM)	$u(h/2)$	0.0198	0.0324	0.5641	1.3758	-113.57
LD4	$u(h/2)$	0.0199	0.0326	0.5659	1.3781	-113.60
ED4(TM)	$w(0)$	-0.1277	-0.7851	-33.011	-226.09	-20294
ED4	$w(0)$	-0.1278	-0.7863	-33.162	-227.02	-20325
ED4(TM)	$u(h/2)$	0.0181	0.0315	0.5638	1.3758	-113.57
ED4	$u(h/2)$	0.0183	0.0317	0.5656	1.3781	-113.60
LD2(TM)	$w(0)$	-0.1610	-0.7921	-33.023	-226.11	-20295
LD2	$w(0)$	-0.1613	-0.7936	-33.174	-227.04	-20325
LD2(TM)	$u(h/2)$	0.0100	0.0296	0.5636	1.3755	-113.57
LD2	$u(h/2)$	0.0102	0.0298	0.5654	1.3778	-113.60
FSDT(TM)	$w(0)$	-0.3484	-0.8567	-32.686	-224.97	-20265
FSDT	$w(0)$	-0.3487	-0.8596	-32.996	-226.88	-20328
FSDT(TM)	$u(h/2)$	0.0062	0.0272	0.5705	1.3837	-113.54
FSDT	$u(h/2)$	0.0062	0.0274	0.5741	1.3887	-113.60
CLT(TM)	$w(0)$	-0.0340	-0.2569	-29.942	-220.30	-20264
CLT	$w(0)$	-0.0344	-0.2600	-30.258	-222.22	-20327
CLT(TM)	$u(h/2)$	0.0081	0.0314	0.5916	1.4231	-113.53
CLT	$u(h/2)$	0.0082	0.0316	0.5952	1.4280	-113.59

The case of the two-layered isotropic shell has been investigated in Table 8 and in Figure 8. The differences in displacements are small, as for the one-layered case: less than 0.5% for both displacement components, and for each thickness ratio and each proposed two-dimensional theory. This small coupling effect is also confirmed in Figure 8, where maximum increment in temperature, of about $0.005\,K$, is obtained for a moderately thin shell. The two layers have different thermal properties, therefore the obtained temperature profile has different slopes in the two considered layers (see Figure 8). The transverse anisotropy, in terms of elastic properties, shows the importance of higher orders of expansion and the inadequacy of CLT and FSDT theories.

Table 9: Three-layered composite shell $(0°/90°/0°)$ with applied mechanical load $p_z = -200000\,Pa$ at the top. Displacements u and w in $[10^{-6}m]$ for several two-dimensional theories and thickness ratios.

	R_α/h	5	10	50	100	1000
LD4(TM)	$w(0)$	-3.6017	-11.130	-231.54	-1050.7	-22017
LD4	$w(0)$	-3.6011	-11.134	-231.68	-1051.2	-22019
LD4(TM)	$u(h/2)$	-0.6829	-0.8937	-12.795	-68.657	-1709.5
LD4	$u(h/2)$	-0.6835	-0.8940	-12.801	-68.683	-1709.5
ED4(TM)	$w(0)$	-3.0467	-10.722	-229.62	-1048.8	-22017
ED4	$w(0)$	-3.0460	-10.727	-229.76	-1049.3	-22018
ED4(TM)	$u(h/2)$	-0.7651	-0.8897	-12.563	-68.437	-1709.4
ED4	$u(h/2)$	-0.7658	-0.8899	-12.569	-68.464	-1709.5
LD2(TM)	$w(0)$	-3.4768	-10.866	-229.17	-1048.5	-22017
LD2	$w(0)$	-3.4761	-10.870	-229.31	-1048.9	-22019
LD2(TM)	$u(h/2)$	-0.7197	-0.8822	-12.664	-68.509	-1709.5
LD2	$u(h/2)$	-0.7203	-0.8824	-12.670	-68.535	-1709.5
FSDT(TM)	$w(0)$	-5.3746	-11.548	-226.46	-1046.3	-22019
FSDT	$w(0)$	-5.3749	-11.550	-226.66	-1047.0	-22021
FSDT(TM)	$u(h/2)$	-0.2143	-0.3783	-12.026	-67.974	-1709.4
FSDT	$u(h/2)$	-0.2142	-0.3781	-12.034	-68.014	-1709.5
CLT(TM)	$w(0)$	-0.2568	-1.9381	-194.08	-1018.0	-22019
CLT	$w(0)$	-0.2571	-1.9406	-194.30	-1018.7	-22021
CLT(TM)	$u(h/2)$	0.0480	0.1177	-0.0973	-65.708	-1709.4
CLT	$u(h/2)$	0.0481	0.1179	-0.0974	-65.751	-1709.4

A three-layered composite shell is investigated in Table 9 and in Figure 9. The small coupling effect is here confirmed by the differences in terms of displacements (less than 0.1%) and the maximum increment in temperature (about $0.01\,K$ for a moderately thin shell). According to these results, the coupling effect in composite materials seems less pronounced than those in isotropic metallic materials. The temperature profile, given in Figure 9, has a less marked zigzag form than the two-layered isotropic shell, because the thermal expansion coefficient α_3 is the same for the three layers, and only the α_1 and α_2 coefficients are exchanged in the embedded layers. The importance of refined theories is clearly shown in Table 9, however CLT and FSDT theories give good results for thin shells ($R_\alpha/h = 1000$).

Table 10: One-layered isotropic shell, free vibrations problem. Fundamental frequency f in Hz for several two-dimensional theories and thickness ratios. Waves number $m = n = 1$. The full coupling problem is indicated with (TM)* in case of imposed temperature conditions and (TM) in case of free temperature conditions.

R_α/h	5	10	50	100	1000
LD4(TM)	1415.3	1238.0	467.78	254.75	84.388
LD4(TM)*	1414.3	1237.0	467.18	254.43	84.365
LD4	1413.5	1235.3	465.79	253.64	84.160
LD2(TM)	1484.8	1284.5	470.43	255.13	84.388
LD2(TM)*	1483.6	1281.9	468.45	254.06	84.323
LD2	1483.5	1281.9	468.42	254.01	84.160
FSDT(TM)	1485.6	1286.0	472.42	256.27	84.617
FSDT	1483.1	1281.0	468.38	254.02	84.161
CLT(TM)	1590.4	1590.4	492.78	259.00	84.618
CLT	1590.4	1590.4	488.19	256.67	84.161

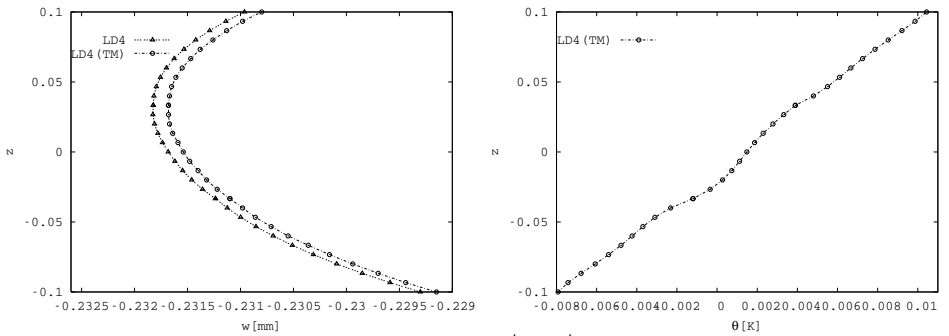

Figure 9: Three-layered composite shell ($0°/90°/0°$) with applied mechanical load $p_z = -200000\ Pa$ at the top. Displacement w and sovra-temperature θ vs. z for $R_\alpha/h = 50$.

In conclusion, the thermo-mechanical coupling effect is very small in the considered shells and can be discarded as already proposed for the plate case given in Brischetto and Carrera (2010). However, fully coupled thermo-mechanical models could be used for future applications, such as thermography investigations [Spiessberger et al. (2008); Fantoni et al. (2008); Ibarra-Castanedo et al. (2008)]: the

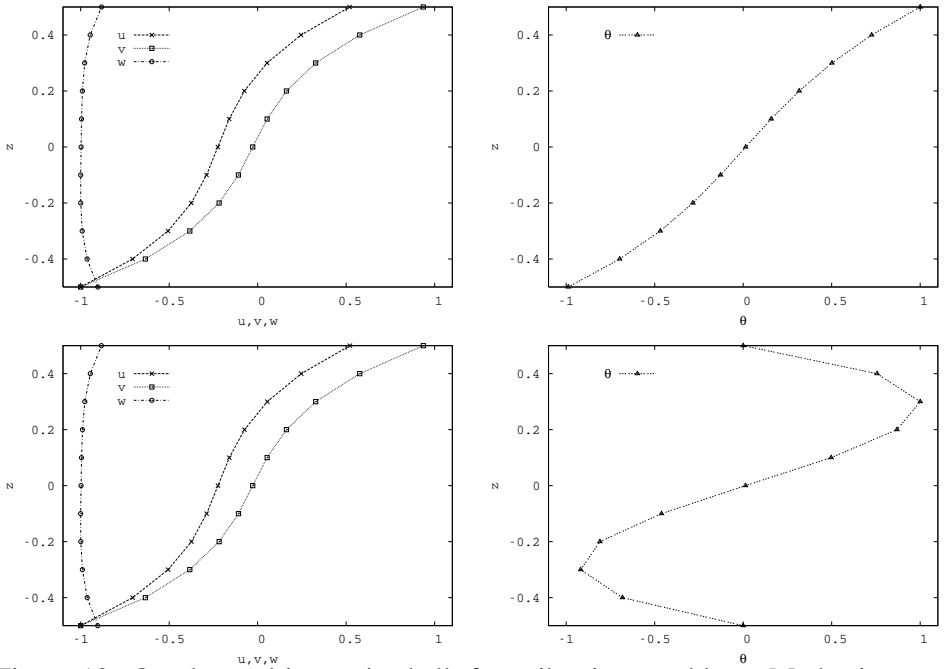

Figure 10: One-layered isotropic shell, free vibrations problem. Modes in terms of displacements and sovra-temperature for the fundamental frequency: $m = n = 1$ and $R_\alpha/h = 10$. LD4 theory for free temperature conditions (top figures) and imposed temperature conditions (bottom figures).

increment in temperature is experimentally measured to determine the strains and stresses which have generated it.

7.3 Free vibrations analysis

Free vibration analysis is investigated for the three proposed simply supported shells. Imposing the wave numbers ($m = n = 1$) in the plane, results are given in terms of fundamental frequency f in Hz. In this dynamic case, the pure mechanical models give smaller frequencies than those obtained with the fully coupled thermo-mechanical models. Table 10 gives the fundamental frequencies for a one-layered isotropic shell, Table 11 for a two-layered isotropic shell, and finally, Table 12 presents results for a three-layered composite shell. The pure mechanical model uses the governing equation (56) and discards the thermal and mechanical loads, while the fully coupled thermo-mechanical model considers the governing equations (71) by discarding the thermal and mechanical loads. In the case of fully

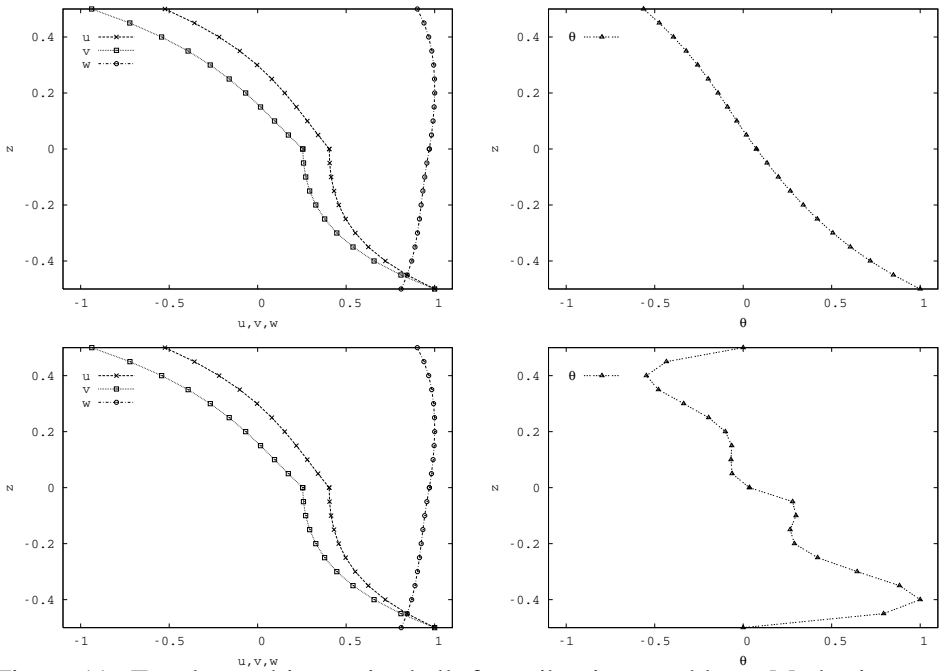

Figure 11: Two-layered isotropic shell, free vibrations problem. Modes in terms of displacements and sovra-temperature for the fundamental frequency: $m = n = 1$ and $R_\alpha/h = 10$. LD4 theory for free temperature conditions (top figures) and imposed temperature conditions (bottom figures).

coupled models, the external surfaces of the plate can have imposed conditions on the sovra-temperature ($\theta_t = \theta_b = 0$, which means the temperature on the external surfaces equals the external room temperature), or no conditions on the sovra-temperature are applied. The first case is here indicated as (TM)*, the second as (TM).

The differences in Table 10 between the pure mechanical fundamental frequency and the fully coupled fundamental frequency are about 0.5% for each investigated thickness ratio and for each proposed two-dimensional theory. The frequencies obtained with the thermo-mechanical models are larger because, when the thermal effect is included, the rigidity matrix undergoes a sort of increase in rigidity. Frequencies obtained with the thermo-mechanical models with imposed thermal conditions (TM)* are smaller than those obtained with free thermal conditions (TM). For classical theories, such as CLT and FSDT, the (TM)* case cannot be considered, because the employed degrees of freedom are not sufficient to impose such

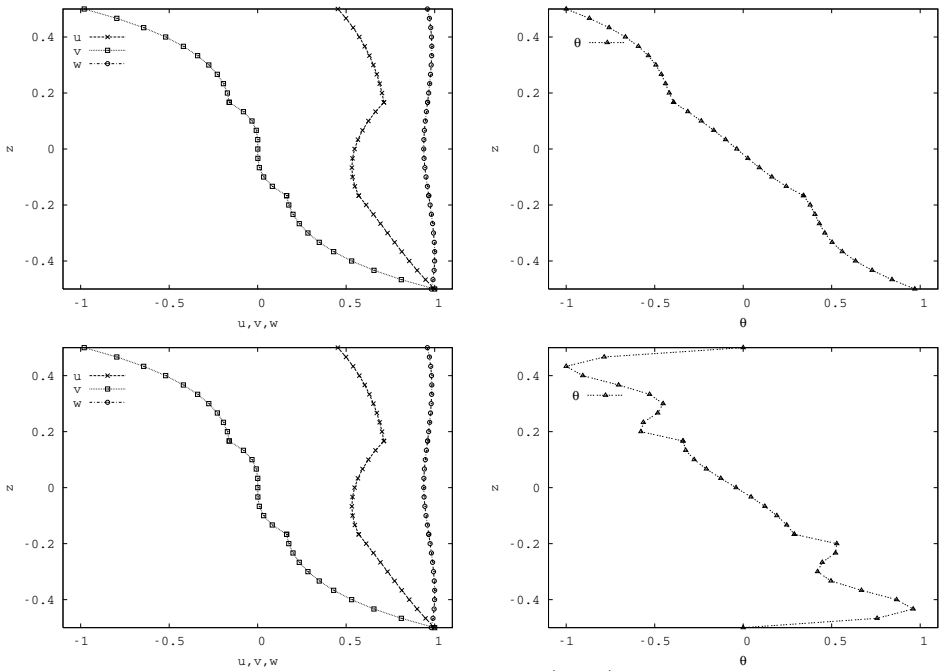

Figure 12: Three-layered composite shell ($0^\circ/90^\circ/0^\circ$), free vibrations problem. Modes in terms of displacements and sovra-temperature for the fundamental frequency: $m = n = 1$ and $R_\alpha/h = 10$. LD4 theory for free temperature conditions (top figures) and imposed temperature conditions (bottom figures).

conditions. CLT and FSDT give good results for thin shells ($R_\alpha/h = 1000$), but CLT(TM) and FSDT(TM) do not properly model the thermal part. Fundamental frequency modes, are given in Figure 10 for both free and imposed thermal conditions, in terms of displacements and temperature, for a thick shell. The first mode is a bending mode, therefore the temperature increases in the compressed part and decreases in the enlarged part of the shell; when the imposed thermal conditions are considered, the sovra-temperature is zero at the top and bottom of the plate. The values given by the modes have only a qualitative sense and they are normalized with the maximum values.

Table 11 proposes the same results as Table 10, but for a two-layered shell. The same conclusions can be drawn: the differences between pure mechanical fundamental frequency and the fully coupled fundamental frequency are less than 0.5%. The importance of refined theories is clearly indicated for thick and moderately thick shells, CLT and FSDT give good results for thin shells ($R_\alpha/h = 1000$), but

Table 11: Two-layered isotropic shell, free vibrations problem. Fundamental frequency f in Hz for several two-dimensional theories and thickness ratios. Waves number $m = n = 1$. The full coupling problem is indicated with (TM)* in case of imposed temperature conditions and (TM) in case of free temperature conditions.

R_α/h	5	10	50	100	1000
LD4(TM)	1372.5	1202.4	455.28	248.41	83.160
LD4(TM)*	1372.3	1202.2	455.15	248.34	83.157
LD4	1371.8	1201.1	454.22	247.89	83.096
ED4(TM)	1378.8	1206.3	455.50	248.44	83.161
ED4(TM)*	1378.7	1206.1	455.37	248.37	83.158
ED4	1378.2	1205.0	454.44	247.93	83.098
LD2(TM)	1395.3	1209.5	455.46	248.43	83.159
LD2(TM)*	1394.8	1208.8	455.06	248.24	83.151
LD2	1394.6	1208.2	454.40	247.92	83.096
FSDT(TM)	1556.3	1257.0	459.28	249.35	83.227
FSDT	1556.3	1254.0	457.10	248.30	83.097
CLT(TM)	1557.6	1559.3	478.65	251.94	83.227
CLT	1557.6	1559.2	476.14	250.84	83.098

they do not properly model the thermal part (see CLT(TM) and FSDT(TM)). The modes, in terms of displacement and temperature, are given in Figure 11 for a thick shell ($R_\alpha/h = 10$); in this case, the transverse anisotropy due to the two different layers is clearly indicated.

A three-layered composite shell is investigated in Table 12 and in Figure 12; the coupling effect is less pronounced than in the other two cases (less than 0.1%) and it disappears for very thin shells ($R_\alpha/h = 1000$). The small coupling is confirmed by the same results obtained with (TM) and (TM)* models. CLT and FSDT give correct results for thin shells ($R_\alpha/h = 1000$). The modes plotted in Figure 12 are for a thick shell ($R_\alpha/h = 10$) and they confirm the transverse anisotropy in a three-layered composite shell. In order to obtain correct values of frequencies for thick shells, higher orders of expansion are necessary.

In conclusion, for the free vibration analysis, the thermo-mechanical coupling effect is very small and it can be discarded. However, fully coupled models are very interesting because they give the modes in terms of displacements and temperature. A possible application could be thermography investigations, as suggested in

Table 12: Three-layered composite shell ($0°/90°/0°$), free vibrations problem. Fundamental frequency f in Hz for several two-dimensional theories and thickness ratios. Waves number $m = n = 1$. The full coupling problem is indicated with (TM)* in case of imposed temperature conditions and (TM) in case of free temperature conditions.

R_α/h	5	10	50	100	1000
LD4(TM)	478.76	452.38	234.37	156.77	108.58
LD4(TM)*	478.75	452.37	234.36	156.77	108.58
LD4	478.67	452.28	234.30	156.74	108.57
ED4(TM)	489.68	457.35	235.36	156.92	108.58
ED4(TM)*	489.67	457.34	235.35	156.91	108.58
ED4	489.57	457.24	235.29	156.88	108.57
LD2(TM)	482.96	458.04	235.59	156.94	108.58
LD2(TM)*	482.92	458.01	235.57	156.93	108.58
LD2	482.87	457.94	235.52	156.91	108.57
FSDT(TM)	513.44	479.34	237.81	157.28	108.58
FSDT	513.42	479.28	237.70	157.22	108.57
CLT(TM)	761.77	759.92	255.58	159.39	108.58
CLT	761.76	759.00	255.44	159.33	108.57

Spiessberger et al. (2008), Fantoni et al. (2008) and Ibarra-Castanedo et al. (2008).

8 Conclusions

A fully coupled thermo-mechanical analysis has been proposed for one-layered and multilayered shells, in analogy with the companion paper [Brischetto and Carrera (2010)], where the same analysis has been performed for plate geometry. The introduction of curvatures for shell geometry, does not add further comments in the conclusions already obtained for the plate case. Both displacements and temperature are considered as primary variables of the problem, and they can be directly obtained from the solution of the governing equations. These features lead to some advantages:

- in the case of an applied temperature to the external surfaces of the shell, the fully coupled analysis permits such values to be easily imposed in the governing equations, and the relative displacements and temperature profile

are directly obtained from the solutions of such equations. The advantages, with respect to a partially coupled thermo-mechanical analysis, have been clearly indicated. In this latter case, in fact, the temperature profile must be a priori defined (assuming it linear in the thickness direction or calculating it by solving the Fourier heat conduction equation) to determine the thermal load;

- in the case of an applied mechanical load to the structure, the fully coupled thermo-mechanical analysis permits the displacement and the temperature generated by the strains to be evaluated. The effect of the thermo-mechanical coupling has been evaluated through comparisons with pure mechanical analysis. The coupling effect is very small and it can therefore be discarded in such an analysis. However, thermo-mechanical coupling could be used for thermography investigations;

- the effect of the thermo-mechanical coupling has also been evaluated for free vibration analysis; the fully coupled thermo-mechanical analysis permits the frequency values and the vibration modes to be evaluated in terms of the displacement and temperature. The effect of thermo-mechanical coupling has also been evaluated for the dynamic case through comparisons with pure mechanical analysis. The coupling effect is very small and it can therefore be discarded in a free vibration analysis. However, thermo-mechanical coupling could be used for thermography investigations, as already suggested for the static case.

Future works will consider the effect of the time evolution of the heat flux, it could be added in the relaxation term to analyze the transient regime of the proposed cases (both plate and shell geometries).

References

Adam, L.; Ponthot, J.-P. (2005): Thermomechanical modeling of metals at finite strains: first and mixed order finite elements. *International Journal of Solids and Structures*, vol. 42, pp. 5615-5655.

Altay, G.A.; Dökmeci, M.C. (1996a): Some variational principles for linear coupled thermoelasticity. *International Journal of Solids and Structures*, vol. 33, pp. 3937-3948.

Altay, G.A.; Dökmeci, M.C. (1996b): Fundamental variational equations of discontinuous thermopiezoelectric fields. *International Journal of Engineering Sci-*

ences, vol. 34, pp. 769-782.

Altay, G.A.; Dökmeci, M.C. (2001): Coupled thermoelastic shell equations with second sound for high-frequency vibrations of temperature-dependent materials. *International Journal of Engineering Sciences*, vol. 38, pp. 2737-2768.

Bhaskar, K.; Varadan, T.K.; Ali, J.S.M. (1996): Thermoelastic solution for orthotropic and anisotropic composite laminates. *Composites. Part B: Engineering*, vol. 27, pp. 415-420.

Birsan, M. (2009): Thermal stresses in cylindrical Cosserat elastic shells. *European Journal of Mechanics - A/Solids*, vol. 28, pp. 94-101.

Brischetto, S.; Leetsch, R.; Carrera, E.; Wallmersperger, T.; Kröplin, B. (2008): Thermo-mechanical bending of functionally graded plates. *Journal of Thermal Stresses*, vol. 31, pp. 286-308.

Brischetto, S. (2009): Effect of the through-the-thickness temperature distribution on the response of layered and composite shells. *International Journal of Applied Mechanics*, vol. 1, pp. 1-25.

Brischetto, S.; Carrera, E. (2009): Thermal stress analysis by refined multilayered composite shell theories. *Journal of Thermal Stresses*, vol. 32, pp. 165-186.

Brischetto, S.; Carrera, E. (2010): Coupled thermo-mechanical analysis of one-layered and multilayered plates. *Composite Structures*, Available online 2 February 2010, doi:10.1016/j.compstruct.2010.01.020.

Cannarozzi, A.A.; Ubertini, F. (2001): A mixed variational method for linear coupled thermoelastic analyis. *International Journal of Solids and Structures*, vol. 38, pp. 717-739.

Carrera, E. (1995): A class of two-dimensional theories for multilayered plates analysis. *Accademia delle Scienze di Torino, Memorie Scienze Fisiche*, vol. 19-20, pp. 1-39.

Carrera, E. (2000): An assessment of mixed and classical theories for the thermal

stress analysis of orthotropic multilayered plates. *Journal of Thermal Stresses*, vol. 23, pp. 797-831.

Carrera, E. (2002): Temperature profile influence on layered plates response considering classical and advanced theories. *AIAA Journal*, vol. 40, pp. 1885-1896.

Carrera, E. (2003): Theories and finite elements for multilayered plates and shells: a unified compact formulation with numerical assessments and benchmarking. *Archivies of Computational Methods in Engineering*, vol. 10, pp. 215-296.

Carrera, E.; Boscolo, M.; Robaldo, A. (2007): Hierarchic multilayered plate elements for coupled multifield problems of piezoelectric adaptice structures: formulation and numerical assessment. *Archives of Computational Methods in Engineering*, vol. 14, pp. 383-430.

Carrera, E.; Brischetto, S. (2008a): Analysis of thickness locking in classical, refined and mixed multilayered plate theories. *Composite Structures*, vol. 82, pp. 549-562.

Carrera, E.; Brischetto, S. (2008b): Analysis of thickness locking in classical, refined and mixed theories for layered shells. *Composite Structures*, vol. 85, pp. 83-90.

Carrera, E.; Brischetto, S.; Nali, P. (2008): Variational statements and computational models for multifield problems and multilayered structures. *Mechanics of Advanced Materials and Structures*, vol. 15, pp. 182-198.

Carrera, E.; Brischetto, S. (2009): Vibrations of plates and shells in the case of thermo-mechanical coupling. In: *The Seventh International Symposium on Vibrations of Continuous Systems*, Zakopane, Poland.

Cauchy, A.L. (1828): Sur l'*é*quilibre et le mouvement d'une plaque solide. *Exercise des Mathématique*, vol. 3, pp. 381-412.

Chao, C.K.; Chen, C.K.; Chen, F.M. (2009): Analytical exact solutions of heat conduction problems for a three-phase elliptical composite. *CMES: Computer Modeling in Engineering & Sciences*, vol. 47, pp. 283-297.

Chen, Z.; Gan, Y.; Chen, J.K. (2008): A coupled thermo-mechanical model for simulating the material failure evolution due to localized heating. *CMES: Computer Modeling in Engineering & Sciences*, vol. 26, pp. 123-137.

Cho, M.; Oh, J. (2004): Higher order zig-zag theory for fully coupled thermoelectric-mechanical smart composite plates. *International Journal of Solids and Structures*, vol. 41, pp. 1331-1356.

Daneshjoo, K.; Ramezani, M. (2002): Coupled thermoelasticity in laminated composite plates based on Green-Lindsay model. *Composite Structures*, vol. 55, pp. 387-392.

Daneshjoo, K.; Ramezani, M. (2004): Classical coupled thermoelasticity in laminated composite plates based on third-order shear deformation theory. *Composite Structures*, vol. 64, pp. 369-375.

Das, N.C.; Das, S.N.; Das, B. (1983): Eigenvalue approach to thermoelasticity. *Journal of Thermal Stresses*, vol. 6, pp. 35-43.

Fantoni, G.; Merletti, L.G.; Salerno, A. (2008): Stato dell'arte della termografia Lock-In applicata a componenti di elicottero: analisi termoelastica e rilevazione di difetti. *Il Giornale delle Prove non Distruttive, Monitoraggio, Diagnostica*, vol. 4, pp. 30-34.

Feng, W.J.; Han, X.; Li, Y.S. (2009): Fracture analysis for two-dimensional plane problems of nonhomogeneous magneto-electro-thermo-elastic plates subjected to thermal shock by using the Meshless Local Petrov-Galerkin method. *CMES: Computer Modeling in Engineering & Sciences*, vol. 48, pp. 1-26.

Givoli, D.; Rand, O. (1994): Dynamic thermoelastic coupling effects in a rod. *AIAA Journal*, vol. 33, pp. 776-778.

Ibarra-Castanedo, C.; Grinzato, E.; Marinetti, S.; Bison, P.; Avdelidis, N.; Grenier, M.; Piau, J.-M.; Bendala, A.; Maldague, X. (2008): Quantitative assessment of aerospace materials by active thermography techniques. In: 9^{th} *International Conference on Quantitative InfraRed Thermography*, Krakow, Poland.

Ibrahimbegovic, A.; Colliat, J.B.; Davenne, L. (2005): Thermomechanical cou-

pling in folded plates and non-smooth shells. *Computer Methods in Applied Mechanics and Engineering*, vol. 194, pp. 2686-2707.

Ikeda, T. (1990): Fundamentals of Piezoelectricity, Oxford University Press, Oxford (UK).

Khare, R.K.; Kant, T.; Garg, A.K. (2003): Closed-form thermo-mechanical solutions of higher-order theories of cross-ply laminated shallow shells. *Composite Structures*, vol. 59, pp. 313-340.

Khdeir, A.A. (1996): Thermoelastic analysis of cross-ply laminated circular cylindrical shells. *International Journal of Solids and Structures*, vol. 33, pp. 4007-4017.

Kirchhoff, G. (1850): *Ü*ber das gleichgewicht und die bewegung einer elastishen scheibe. *Journal fur die reine und Angewandte Math*, vol. 40, pp. 51-88.

Kosinski, W.; Frischmuth, K. (2001): Thermomechanical coupled waves in a nonlinear medium. *Wave Motion*, vol. 34, pp. 131-141.

Lee, Z.-Y. (2006): Generalized coupled transient thermoelastic problem of multilayered hollow cylinder with hybrid boundary conditions. *International Communications in Heat and Mass Transfer*, vol. 33, pp. 518-528.

Leissa, A.W. (1973): Vibration of Shells, NASA SP-288, Washington, D.C. (USA).

Librescu, L.; Marzocca, P. (2003a): Thermal Stresses'03, vol.1, Virginia Polytechnic Institute and State University, Blacksburg, VA(USA).

Librescu, L.; Marzocca, P. (2003b): Thermal Stresses'03, vol.2, Virginia Polytechnic Institute and State University, Blacksburg, VA(USA).

Liu, D.; Zheng, X.; Liu, Y. (2009): A discontinuous Galerkin Finite Element Method for heat conduction problems with local high gradient and thermal contact resistance. *CMES: Computer Modeling in Engineering & Sciences*, vol. 39, pp. 263-299.

Mindlin, R.D. (1951): Influence of rotatory inertia and shear in flexural motions of isotropic elastic plates. *Journal of Applied Mechanics*, vol. 18, pp. 31-38.

Noor, A.K.; Burton, W.S. (1992): Computational models for high-temperature multilayered composite plates and shells. *Applied Mechanics Reviews*, vol. 45, pp. 419-446.

Noorzaei, J.; Bayagoob, K.H.; Abdulrazeg, A.A.; Jaafar, M.S.; Mohammed, T.A. (2009): Three dimensional nonlinear temperature and structural analysis of roller compacted concrete dam. *CMES: Computer Modeling in Engineering & Sciences*, vol. 47, pp. 43-60.

Nowinski, J.L. (1978): Theory of Thermoelasticity with Applications, Sijthoff & Noordhoff, The Netherlands.

Oh, J.; Cho, M. (2004): A finite element based on cubic zig-zag plate theory for the prediction of thermo-electric-mechanical behaviors. *International Journal of Solids and Structures*, vol. 41, pp. 1357-1375.

Poisson, S.D. (1829): M*é*moire sur l'*é*quilibre et le mouvement des corps *é*lastique. *Mémoires de l'Académie des Sciences des Paris*, vol. 8, pp. 357-570.

Reddy, J.N. (2004): Mechanics of Laminated Composite Plates and Shells. Theory and Analysis, CRC Press, New York (USA).

Rolfes, R.; Noack, J.; Taeschner, M. (1999): High performance 3D-analysis of thermo-mechanically loaded composite structures. *Composite Structures*, vol. 46, pp. 367-379.

Sladek, J.; Sladek, V.; Solek, P.; Wen, P.H. (2008a): Thermal bending of Reissner-Mindlin plates by the MLPG. *CMES: Computer Modeling in Engineering & Sciences*, vol. 28, pp. 57-76.

Sladek, J.; Sladek, V.; Solek, P.; Wen, P.H.; Atluri, S.N. (2008b): Thermal analysis of Reissner-Mindlin shallow shells with FGM properties by the MLPG. *CMES: Computer Modeling in Engineering & Sciences*, vol. 30, pp. 77-97.

Sladek, J.; Sladek, V.; Tan, C.L.; Atluri, S.N. (2008c): Analysis of transient heat conduction in 3D anisotropic functionally graded solids by the MLPG method. *CMES: Computer Modeling in Engineering & Sciences*, vol. 32, pp. 161-174.

Sladek, J.; Sladek, V.; Solek, P.; Tan, C.L.; Zhang, C. (2009): Two and three-dimensional transient thermoelastic analysis by the MLPG method. *CMES: Computer Modeling in Engineering & Sciences*, vol. 47, pp. 61-95.

Spiessberger, C.; Gleiter, A.; Busse, G. (2008): Aerospace applications of lockin-thermography with optical, ultrasonic and inductive excitation. In: *International Symposium on NDT in Aerospace*, Fürth, Germany.

Tanaka, M.; Matsumoto, T.; Moradi, M. (1995): Application of boundary element method to 3-D problems of coupled thermoelasticity. *Engineering Analysis with Boundary Elements*, vol. 16, pp. 297-303.

Trajkoviski, D.; Cukic, R. (1999): A coupled problem of thermoelastic vibrations of a circular plate with exact boundary conditions. *Mechanics Research Communications*, vol. 26, pp. 217-224.

Wauer, J. (1996): On magneto-thermo-elastic vibrations. *Journal of Thermal Stresses*, vol. 19, pp. 671-691.

Wilms, E.V.; Cohen, H. (1985): Some one-dimensional problems in coupled thermoelasticity. *Mechanics Research Communication*, vol. 12, pp. 41-47.

Wu, X.H.; Shen, S.P.; Tao, W.Q. (2007): Meshless Local Petrov-Galerkin Collocation method for two-dimensional heat conduction problems. *CMES: Computer Modeling in Engineering & Sciences*, vol. 22, pp. 65-76.

Wu, Z.; Chen, W. (2008): A global-local higher order theory for multilayered shells and the analysis of laminated cylindrical shell panels. *Composite Structures*, vol. 84, pp. 350-361.

Yang, Q.; Stainer, L.; Ortiz, M. (2006): A variational formulation of the coupled thermo-mechanical boundary-value problem for general dissipative solids. *Journal of the Mechanics and Physics of Solids*, vol. 54, pp. 401-424.

Yeh, Y.-L. (2005): The effect of thermo-mechanical coupling for a simply supported orthotropic rectangular plate on non-linear dynamics. *Thin-Walled Structures*, vol. 43, pp. 1277-1295.

Zhou, Y.; Li, X.; Yu, D. (2009): Transient thermal response of a partially insulated crack in an orthotropic functionally graded strip under convective heat supply. *CMES: Computer Modeling in Engineering & Sciences*, vol. 43, pp. 191-221.